Biogeochemical processes captured by carbon isotopes in redox-stratified water columns: a comparative study of four modern stratified lakes along an alkalinity gradient

Robin Havas[1], Christophe Thomazo[1,2], Miguel Iniesto[3], Didier Jézéquel[4,5], David Moreira[3], Rosaluz Tavera[6], Jeanne Caumartin[7], Elodie Muller[7], Purificación López-García[3], and Karim Benzerara[7]

[1]Biogéosciences, CNRS, Université Bourgogne Franche-Comté, 21000 Dijon, France
[2]Institut Universitaire de France, 75005 Paris, France
[3]Ecologie Systématique Evolution, CNRS, Université Paris-Saclay, AgroParisTech, 91190 Gif-sur-Yvette, France
[4]IPGP, CNRS, Université de Paris Cité, 75005 Paris, France
[5]UMR CARRTEL, INRAE and USMB, 74200 Thonon-les-Bains, France
[6]Departamento de Ecología y Recursos Naturales, Universidad Nacional Autónoma de México, Mexico City, México
[7]Institut de Minéralogie, de Physique des Matériaux
et de Cosmochimie (IMPMC), CNRS, Muséum National d'Histoire Naturelle, Sorbonne Université, 75005 Paris, France

Correspondence: Robin Havas (robin.havas@gmail.com)

Abstract. Redox-stratified water columns are a prevalent feature of the Earth's history, and ongoing environmental changes tend to promote a resurgence of such settings. Studying modern redox-stratified environments has improved our understanding of biogeochemical processes and element cycling in such water columns. These settings are associated with peculiar carbon biogeochemical cycling, owing to a layered distribution of biological processes in relation to oxidant availability. Metabolisms from distinct biogeochemical layers are diverse and may differently imprint the sedimentological record. Paired carbon isotope compositions of organic matter and carbonates, which are commonly used to characterize these ecological dynamics, can thus vary from one stratified environment to another. Changes in the organic/inorganic carbon sources and mass balance can further complicate the isotopic message in stratified environments. Better understanding of these multifaceted carbon isotope signals requires further evaluation of how the processes occurring in redox-stratified water columns are transferred to the sediments. We therefore characterized and compared the isotopic signatures of dissolved inorganic carbon (DIC), carbonate, and organic matter reservoirs at different depths in the water column and upper sediments of four stratified Mexican lakes that follow a gradient of alkalinity and salinity. Comparing these systems shows strong diversity in the carbon isotope signals of the water column and sediments. Differences in inorganic carbon isotope signatures arise primarily from the size of the DIC reservoir, buffering the expression of redox-dependent biological processes as alkalinity increases. Combining this isotopic dataset with water column physicochemical parameters allows us to identify oxygenic photosynthesis and aerobic respiration in the four lakes studied, while anoxygenic photosynthesis is evidenced in only two of them. Sedimentary organic matter does not originate from the same water column layers in the four lakes, highlighting the ecological variability that can stem from different stratified water columns and how it is transferred or not to the sedimentary record. The least alkaline lake shows higher isotopic variability and signatures typical of methanogenesis in the sediment porewaters. This metabolism, however, does not leave diagnostic isotopic signatures in the sedimentary archives (organic matter and carbonates), underlining the fact that even when alkalinity does not strongly buffer the inorganic carbon reservoir, a comprehensive picture of the active biogeochemical carbon cycling is not necessarily transferred to the geological record.

1   Introduction

The carbon cycle and biogeochemical conditions prevailing at the surface of the Earth are intimately bound through biological (e.g., photosynthesis) and geological processes (e.g., volcanic degassing and silicate weathering). The analysis of carbon isotopes in organic matter and carbonates ($\delta^{13}C_{org}$ and $\delta^{13}C_{carb}$) in the rock record has been used to reconstruct the evolution of the biosphere and the oxygenation of the Earth's surface (e.g., Hayes et al., 1989; Karhu and Holland, 1996; Schidlowski, 2001). Coupling $\delta^{13}C_{org}$-$\delta^{13}C_{carb}$ has frequently been used to infer the burial rate of organic C and thus the redox balance of the atmosphere and hydrosphere (e.g., Karhu and Holland, 1996; Aharon, 2005; Krissansen-Totton et al., 2015; Mason et al., 2017). It has also been used to deduce the presence of metabolisms like anoxygenic chemoautotrophic or methanotrophic bacteria (e.g., Hayes et al., 1999; Bekker et al., 2008; Krissansen-Totton et al., 2015). Coupling $\delta^{13}C_{org}$-$\delta^{13}C_{carb}$ has also been used to discuss ocean stratification and its effect on inorganic and organic C geochemical signatures in sediments (e.g., Logan et al., 1995; Aharon, 2005; Bekker et al., 2008; Ader et al., 2009). Stratification favors the expression and recording of different layers of the water column, with potentially very distinct isotopic signatures. As the oceans were redox stratified during most of the Earth's history (Lyons et al., 2014; Havig et al., 2015; Satkoski et al., 2015), processes affecting the C cycle were likely different from those occurring in most modern, well-oxygenated environments. This change of conditions could impact the $\delta^{13}C_{org}$ signal at various scales, from changes in diversity and relative abundance of microbial carbon and energy metabolism (e.g., Wang et al., 2016; Iñiguez et al., 2020; Hurley et al., 2021) to larger ecological interactions (e.g., Jiao et al., 2010; Close and Henderson, 2020; Klawonn et al., 2021) and global C dynamics (e.g., Ridgwell and Arndt, 2015; Ussiri and Lal, 2017).

Modern stratified lakes have been used as analogues of ancient redox-stratified systems to better understand the C cycle in the sedimentary isotopic record (e.g., Lehmann et al., 2004; Posth et al., 2017; Fulton et al., 2018). Several recent studies have investigated the C cycle in modern stratified water columns (e.g., Crowe et al., 2011; Kuntz et al., 2015; Posth et al., 2017; Schiff et al., 2017; Havig et al., 2018; Cadeau et al., 2020; Saini et al., 2021; Petrash et al., 2022), where many biogeochemical and physicochemical parameters can be directly measured, together with the main C reservoirs. However, investigations of such Precambrian analogues do not necessarily include sediment data and generally focus on a single environment without integrating views from several systems.

In this study, we measured the concentrations and isotopic compositions of dissolved inorganic carbon (DIC) and particulate organic carbon (POC) throughout the water column of four modern redox-stratified alkaline crater lakes, located in the Trans-Mexican Volcanic Belt (Ferrari et al., 2012). We also measured the concentrations and isotopic compositions of the sedimentary organic carbon and carbonates as well as porewater DIC from surficial sediments ($\sim 10\,cm$) at the bottom of the lakes. The four lakes share similar geological and climatic contexts but have distinct solution chemistries along a marked alkalinity–salinity gradient (Zeyen et al., 2021) – as well as distinct planktonic communities (Iniesto et al., 2022). We therefore seek to evaluate how these environmental and ecological differences are recorded in the C isotope signatures in the water columns (DIC–POC) and sedimentary archives (organic matter–carbonates). The four lakes are closed lakes in endorheic basins (Alcocer, 2021; Zeyen et al., 2021), which facilitates the identification of external environmental constraints (e.g., evaporation, C sources) and their influence on processes occurring within the water columns. Depth profiles of the main physicochemical parameters together with trace and major element concentrations were measured to pinpoint the dominant biogeochemical processes occurring in the water columns and link them to specific C isotopes signatures.

First, we constrain the main DIC sources and external controls on the lakes' alkalinities. Next, we describe the influence of the inter-lake alkalinity gradient on the inorganic C cycle and stratification of the lakes and how it is recorded in surficial sediments. Then, by combining POC and DIC data, we identify the sources of organic C to the lakes by describing the main autotrophic reactions occurring in the water columns (e.g., oxygenic and anoxygenic photosynthesis). Finally, we discuss the fate of POC, either recycled (e.g., via methanogenesis) or deposited in the sediments, and how all these processes are recorded (or not) in surficial sediments.

2   Setting and context

2.1   Geology

The four lakes studied here are volcanic tuff cones and maars formed after phreatic, magmatic, and phreatomagmatic explosions, related to volcanic activity in the Trans-Mexican Volcanic Belt (TMVB, Fig. 1). The TMVB originates from the subduction of the Rivera and Cocos plates beneath the North American plate, resulting in a long ($\sim 1000\,km$) and wide (90–230 km) Neogene volcanic arc spreading across central Mexico (Ferrari et al., 2012). The TMVB harbors a large variety of monogenetic scoria cones and phreatomagmatic vents (maars and tuff cones) as well as stratovolcanoes, calderas, and domes (Carrasco-Núñez et al., 2007; Ferrari et al., 2012; Siebe et al., 2014). Maar crater formation usually occurs when ascending magma meets water-saturated substrates, leading to successive explosions and the excavation of older units (Lorenz, 1986; Carrasco-Núñez et al., 2007; Siebe et al., 2012; Chako Tchamabé et al., 2020).

The first lake, Alberca de los Espinos (1985 m a.s.l.), is located at the margin of the Zacapu tectonic lacustrine basin

in the Michoacán–Guanajuato volcanic field (MGVF) in the central western part of the TMVB (Fig. 1). It lies on andesitic basement rocks and was dated at $\sim 25 \pm 2$ ka (Siebe et al., 2012, 2014). The other three lakes (La Preciosa, Atexcac, and
5 Alchichica) are all in the same area (~ 50 km^2) of the Serdán-Oriental basin (SOB) in the easternmost part of the TMVB (Fig. 1). The SOB is a closed intra-montane basin at high altitude (~ 2300 m), surrounded by the Los Humeros caldera to the north and the Cofre de Perote–Citlatépetl volcanic range
10 to the east. The basement is composed of folded and faulted Cretaceous limestones and shales, covered by andesitic-to-basaltic lava flows (Carrasco-Núñez et al., 2007; Armienta et al., 2008; Chako Tchamabé et al., 2020). The Alchichica and Atexcac craters was dated at ~ 6–13 ± 5–6 ka (Chako
15 Tchamabé et al., 2020) and 330 ± 80 ka (Carrasco-Núñez et al., 2007), respectively (Table 1). The age of La Preciosa is not known.

2.2 Climate and limnology

Alberca is a freshwater lake (0.6 psu) with a temperate to
20 semi-humid climate (Rendon-Lopez, 2008; Sigala et al., 2017). In contrast, lakes from the SOB experience a similar temperate to semi-arid climate (Armienta et al., 2008; Sigala et al., 2017). The current climate of the SOB is dominated by dry conditions, reflected by higher evaporation than precip-
25 itation fluxes in Lake Alchichica (~ 1686 vs. 392 mm yr^{-1}; Alcocer, 2021). In La Preciosa, Atexcac, and Alchichica, significant evaporation is reflected by a drop in water level, evidenced by the emersion of microbialite deposits (Fig. S1; Zeyen et al., 2021). This evaporation-dominated climate
30 strongly contributes to the relatively high salinity values in these lakes (1.2–7.9 psu), ranging from sub- to hyposaline.

The four lakes are warm monomictic: they are stratified for about 9 months of the year, mixing only when thermal stratification breaks down in the cold of winter (Armienta et
35 al., 2008). They are all closed lakes located in an "endorheic" basin (Alcocer, 2021; Zeyen et al., 2021), meaning that they have no inflow, outflow, or connection to other basins through surficial waters such as streams. The only water input is from precipitation and groundwater inflow (quantified for Lake
40 Alchichica; Alcocer, 2021, and references therein).

The four lakes are alkaline (pH ~ 9) but cover a broad range of chemical compositions (including alkalinity, salinity, and Mg / Ca ratio), interpreted as reflecting different concentration stages of an initial alkaline dilute water (Table 1;
45 Zeyen et al., 2021). Variations in concentration stages may be due to differences in climate and, more generally, different hydrological regimes. Microbialite deposits are found in all four lakes (Gérard et al., 2013; Saghaï et al., 2016; Iniesto et al., 2021a, b; Zeyen et al., 2021) and increase in abun-
50 dance from lower to higher alkalinity conditions (Zeyen et al., 2021).

3 Method

3.1 Sample collection

The sediment core from Lake La Preciosa was collected in May 2016. All other samples were collected in May 2019.
55 The depth profiles of several physicochemical parameters were measured in the water columns of the four lakes using an YSI EXO2 Multiparameter probe: temperature, pH, ORP (oxidation reduction potential), conductivity, O$_2$, chlorophyll a, phycocyanin, and turbidity. Precisions for these mea-
60 surements were 0.01 °C, 0.1 pH unit, 20 mV, 0.001 mS cm^{-1}, 0.1 mg L^{-1}, 0.01 µg L^{-1}, 0.01 µg L^{-1} and 2 % FTU (formazine turbidity unit), respectively. The ORP signal was not calibrated before each profile and is thus used to discuss relative variations over a depth profile. Measurements
65 of the aforementioned parameters served to pinpoint depths of interest for further chemical and isotopic analyses, notably around the redoxcline of the lakes. Water samples were collected with a Niskin bottle. Particulate matter was collected on pre-combusted (2 h at 490 °C) and weighted glass fiber
70 filters (Whatman GF/F, 0.7 µm) and analyzed for particulate organic carbon (POC), major elements, and trace elements. Between 1.5 and 5 L of lake water was filtered before the GF/F filters became clogged. The processed solution was filtered again at 0.22 µm with Filtropur S filters (pre-rinsed with
75 lake water filtered at 0.7 µm) for analyses of dissolved inorganic carbon (DIC) and major, minor, and trace ions.

Sediment cores were collected using a 90 mm UWITEC corer close to the deepest point of each lake's water column (Table 1), where anoxic conditions prevail almost all
80 year long. Cores measured between 20 and 85 cm in length. Slices of about 2–3 cm were cut under anoxic conditions, using a glove bag filled with N$_2$ (anoxia was monitored using a WTW3630 equipped with a FDO O$_2$ Optode). Interstitial porewater was drained out of the core slices using Rhizons
85 in the glove bag. Sediments were transported back to the laboratory within aluminized foils (Protpack, UK). Sediments were then fully dried in a laboratory anoxic N$_2$-filled glove box.

3.2 Dissolved inorganic carbon (DIC) concentration
90 and isotope measurements

Of the 0.7 µm filtered lake water, 12 mL was filtered at 0.22 µm directly into hermetic Exetainer® tubes to avoid exchange between DIC and atmospheric CO$_2$. The DIC concentrations and isotopic compositions were measured at the
95 Institut de Physique du Globe de Paris (IPGP, France), using an Analytical Precision 2003 GC-IRMS (gas chromatography isotope-ratio mass spectrometry), running under He continuous flow, following the protocol described by Assayag et al. (2006). A given volume of the solution was extracted from
100 the Exetainer® tube with a syringe, while the same volume of helium was introduced to maintain stable pressure and
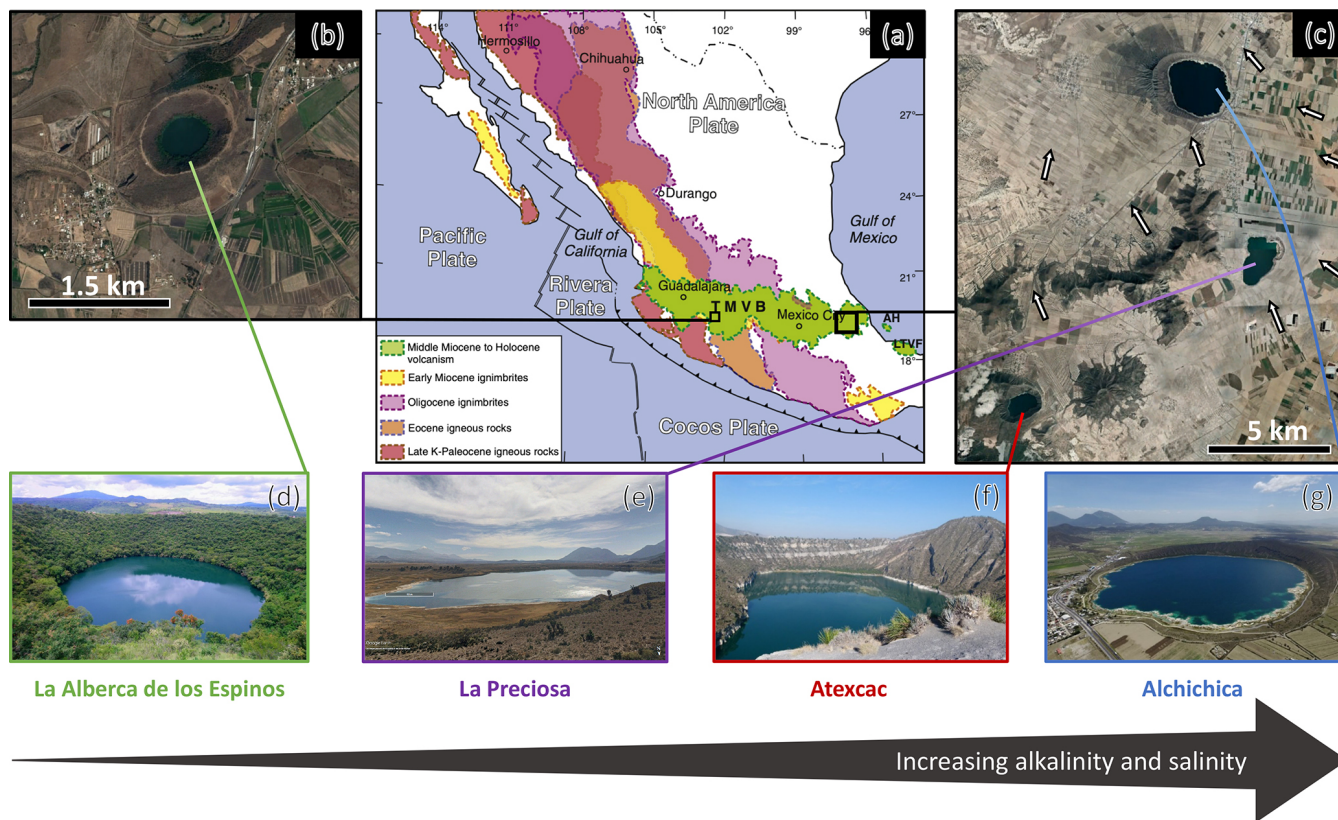
Figure 1. [TS1] Geographical location and photographs of the four crater lakes. **(a)** Geological map from Ferrari et al. (2012), with black squares showing the location of the four studied lakes within the Trans-Mexican Volcanic Belt (TMVB). **(b, c)** Close up © Google Earth views of Alberca de los Espinos and the Serdán-Oriental basin (SOB). The white arrows represent the approximate groundwater flow path (based on Silva-Aguilera, 2019). **(d–g)** Photographs of the four lakes (panel **d** from © Google Image ["enamoratedemexicowebsite"], panel **e** from © Google Earth street view, and panel **g** from © "Agencia Es Imagen").

atmospheric-CO_2-free conditions within the sample tubes. The collected sample was inserted into another Exetainer® tube, pre-filled with a few drops of 100 % phosphoric acid (H_3PO_4), and pre-flushed with He gas. Under acidic conditions, DIC quantitatively converts to gaseous and aqueous CO_2, which equilibrates overnight within the He-filled head space of the tube. Quantification and isotopic analyses of released gaseous CO_2 were then carried out by GC-IRMS using internal standards of known composition that were prepared and analyzed via the same protocol. Each measurement represented an average of four injections in the mass spectrometer. Chemical preparation and IRMS analysis were duplicated for all the samples. The $\delta^{13}C_{DIC}$ reproducibility calculated for the 65 samples was better than $\pm 0.2\,‰$, including internal and external reproducibility. Standard deviation for [DIC] was $0.6 \pm 0.9\,\mathrm{mmol\,L^{-1}}$ on average.

Specific DIC speciation, i.e., $CO_{2(aq)}$, HCO_3^-, and CO_3^{2-} activities, was computed using PHREEQC with the full dissolved chemical composition of each sample as an input. It should be noted that these results are calculated from theoretical chemical equilibria and do not necessarily take into account local kinetic effects, which, for example, could lead to local exhaustion of $CO_{2(aq)}$ where intense photosynthesis occurs.

3.3 Particulate organic carbon and nitrogen (POC, PON)

Particulate organic matter from the lake water columns was collected on GF/F filters, dried at room temperature, and ground in a ball mill before and after decarbonation. Decarbonation was performed with 12N HCl vapors in a desiccator for 48 h. Aliquots of dry decarbonated samples (25–70 mg) were weighed in tin capsules. The POC and PON contents and $\delta^{13}C_{POC}$ were determined at the Laboratoire Biogéosciences (Dijon, France) using a Vario Micro Cube elemental analyzer (Elementar, Hanau, Germany) coupled with an Iso-Prime IRMS (Isoprime, Manchester, UK) in continuous flow mode. The USGS40 and IAEA-600 certified materials used for calibration showed reproducibility better than 0.15 ‰ for $\delta^{13}C$. External reproducibility based on triplicate analyses of samples ($n = 23$) was 0.1 ‰ on average for $\delta^{13}C_{POC}$ (1SD). External reproducibility for POC and PON concentrations

Table 1. General information about the lakes studied. Abbreviations: TMVB, Trans-Mexican Volcanic Belt; MGVF, Michoacán–Guanajuato volcanic field; m a.s.l., meters above sea level. *NB*: Sampling took place in May 2019, except for the La Preciosa sediments sampled in May 2016.

Lake	General location	Sampling location	Elevation (m a.s.l.)	Lake basement	Age	Max depth (m)	Alkalinity (mmol L^{-1})	Salinity (psu)	pH
Alchichica	Serdán–Oriental basin, eastern TMVB	19°24′51.5″ N; 97°24′09.9″ W	2320	Limestone, basalts	6–13 ± 5–6 ka	63	~35	7.9	9.22
Atexcac	Serdán–Oriental basin, eastern TMVB	19°20′2.2″ N; 97°26′59.3″ W	2360	Limestone, andesites, basalts	330 ± 80 ka TS2	39	~26	7.4	8.85
La Preciosa	Serdán–Oriental basin, eastern TMVB	19°22′18.1″ N; 97°23′14.4″ W	2330	Limestone, basalts	Pleistocene TS3	46	~13.5	1.15	9.01
Alberca de los Espinos	Zacapu basin, MGVF, central TMVB	19°54′23.9″ N; 101°46′07.8″ W	1985	Andesite	25 ± 2 ka	30	~7	0.6	9.14

was 0.001 and 0.005 mmol L^{-1} on average, respectively (i.e., 3 % and 7 % of measured concentrations).

3.4 Geochemical characterizations of the sediments

Sedimentary organic carbon (SOC), sedimentary organic nitrogen (SON), and their isotopic compositions were measured on carbonate-free residues of the first 12 cm of the sediment cores, produced after overnight 1N HCl digestion. Plant debris (mainly found in Alberca and Atexcac) was identified upon initial sediment grinding in an agate mortar and analyzed separately. Aliquots of dried decarbonated samples ($\sim$ 4–70 mg) were weighed in tin capsules. The SOC and SON contents and δ^{13}C were determined at the Laboratoire Biogéosciences (Dijon) using a Vario Micro Cube elemental analyzer (Elementar GmbH, Hanau, Germany) coupled with an IsoPrime IRMS (Isoprime, Manchester, UK) in continuous flow mode. The USGS40 and IAEA-600 certified materials used for calibration had a reproducibility better than 0.2 ‰ for δ^{13}C$_{SOC}$. Sample analyses ($n = 67$) were at least duplicated and showed an average external reproducibility of 0.1 ‰ for δ^{13}C (1SD). External reproducibility for SOC and SON contents was 0.1 wt % and 0.03 wt %, respectively.

Carbon isotope compositions of sedimentary carbonates were analyzed at the Laboratoire Biogéosciences (Dijon) using a Thermo Scientific™ DELTA V Plus™ IRMS coupled with a Kiel IV carbonate device. External reproducibility was assessed by multiple measurements of NBS19 standard and was better than $\pm$ 0.1 ‰ (2σ). Total carbonate concentration was determined by mass balance after decarbonatation for SOC analysis.

Mineralogical assemblages of sediments were determined on bulk powders by X-ray diffraction (XRD) at the Laboratoire Biogéosciences (Dijon). Samples were ground in an agate mortar. Diffractograms were obtained with a Bruker D8 ENDEAVOR diffractometer, with CuKα radiation and LYNXEYE XE-T detector, under 40 kV and 25 mA intensity. Mineral identification was based on the COD ("Crystallography Open Database") and BGMN databases. Mineral abundances were estimated by Rietveld refinement analysis implemented in the Profex software.

Solid sulfide concentrations were determined on dry bulk sediments from Lake Alberca after a wet chemical extraction using a boiling acidic Cr(II) solution, as detailed in Gröger et al. (2009).

3.5 Major and trace element concentrations

Dissolved and particulate matter elemental compositions were measured at the Pôle Spectrométrie Océan (Plouzané, France) by inductively coupled plasma–atomic emission spectroscopy (ICP-AES, Horiba Jobin) for major elements and by high-resolution ICP–mass spectrometry using an Element XR (HR-ICP-MS, Thermo Fisher Scientific) for trace elements. Major element measurement reproducibility based

on internal multi-elemental solution was better than 5 %. Trace elements were analyzed by a standard sample bracketing method and calibrated with a multi-elemental solution. Analytical precision for trace elements was generally better than 5 %. Dissolved sulfate concentrations were analyzed by ion chromatography at the IPGP (Paris, France), with uncertainty lower than 5 %.

4 Results

4.1 Lake Alberca de los Espinos

Stratification of the water column was well defined in Alberca de los Espinos (Fig. 2). Temperature was higher than in the other lakes (decreasing from $\sim 23\,°C$ at the surface to $16.5\,°C$ at depth). Dissolved O_2 was oversaturated at the lake surface (118 %, i.e., $7.9\,mg\,L^{-1}$), rapidly decreasing to 0 between ~ 5 and 12 m, while the oxidation reduction potential (ORP) only decreased below 17 m depth. The offset between O_2 exhaustion and ORP decrease can be explained by the presence of other oxidant species and/or extended chlorophyll a peaks (Supplement Text S1). Conductivity decreased from 1.20 to $1.17\,mS\,cm^{-1}$ at 16 m before increasing to $1.27\,mS\,cm^{-1}$ at 26 m (salinity between 0.58 and 0.64 psu). Chlorophyll a (Chl a) averaged $3.1\,\mu g\,L^{-1}$, and showed a profile with at least three distinctive peaks, (i) between 6 and 9.5 m, (ii) around 12.5 m, and (iii) between 16 and 19 m, all reaching $\sim 4\,\mu g\,L^{-1}$. The turbidity profile showed a pronounced increase from 16 to 19 m. The pH profile showed important variation from 9.15 at the lake surface to 8.75 between 6.5 and 10 m, further decreasing to 7.5 between 16 and 26 m. Based on the temperature profiles, epilimnion, metalimnion, and hypolimnion layers of Lake Alberca de los Espinos in May 2019 broadly extended from 0–5, 5–12, and 12–30 m, respectively (Fig. 2). The conductivity and pH profiles, however, show that different conditions prevail at the top and bottom of the hypolimnion.

Dissolved inorganic carbon (DIC) concentration progressively increased from 6.8 mM at 5 m to 8.7 mM at 26 m. The $p\mathrm{CO}_2$ calculated for surface waters was near equilibrium with atmospheric $p\mathrm{CO}_{2\,atm}$ but strongly increased with depth, up to ~ 40 times the $p\mathrm{CO}_{2\,atm}$ (Table S2). The $\delta^{13}C_{DIC}$ first decreased from about $-2.5\,‰$ to $-4.1\,‰$ between 5 and 10 m, before increasing again up to $-2\,‰$ at 25 m. Particulate organic carbon (POC) concentrations reached minimum values of 0.02 mM at 10 m but rose to maximum values in the hypolimnion (0.06 mM). The C : N molar ratio of particulate organic matter (POM) progressively decreased from 8.5 at the surface to less than 6.5 in the hypolimnion. The $\delta^{13}C_{POC}$ had minimum values at 10 and 17 m ($-28.3\,‰$ and $-29\,‰$, respectively). Above and below these depths, $\delta^{13}C_{POC}$ averaged $-26.4 \pm 0.5\,‰$.

Dissolved sulfates as measured by chromatography were only detectable at 5 m, with a low concentration of $12\,\mu M$, while total dissolved S measured by ICP-AES showed values in the hypolimnion higher than in the upper layers (~ 10.3 vs. $7.4\,\mu M$, Table S4). Dissolved Mn concentrations decreased from 1.5 to $0.5\,\mu M$ between 5 and 10 m, then increased to $2\,\mu M$ at 25 m. Aqueous Fe was only detectable at 25 m, with a concentration of $0.23\,\mu M$ (Table S4). In parallel, particulate S concentrations increased with depth, with a marked increase from 0.1 to $0.6\,\mu M$ between 20 and 25 m. Increase in particulate S was correlated with a 25-fold increase in particulate Fe (from 0.2 to $5.97\,\mu M$). Particulate Mn showed a peak between 17 and 20 m around $1\,\mu M$, contrasting with values lower than $0.15\,\mu M$ in the rest of the water column (Fig. 2, Table S5).

In the first centimeters of sediments, DIC concentration in the porewater varied between ~ 11 and 12 mM, and $\delta^{13}C_{DIC}$ varied between $+8\,‰$ and $+10\,‰$ (Figs. 3, 4). Surficial sedimentary carbonates corresponded to calcite and had a $\delta^{13}C$ around $-1.5\,‰$. Sedimentary organic matter had a $\delta^{13}C_{SOC}$ increasing from $\sim -29.4\,‰$ to $-25.5\,‰$ and a C : N molar ratio varying between 11.6 and 14.3 (Figs. 3, 4; Table S3).

4.2 Lake La Preciosa

Lake La Preciosa was also stratified at the time of sample collection (Fig. 2). Temperature decreased from $\sim 20\,°C$ at the surface to $16\,°C$ at 15 m depth. Conductivity showed the same trend with values between 2.24 and $2.22\,mS\,cm^{-1}$ (salinity around 1.15 psu). Dissolved O_2 was oversaturated at the lake surface (120 %, i.e., $8.4\,mg\,L^{-1}$), rapidly decreasing to 0 between ~ 8 and 14 m, while the ORP decreased right below 16 m. Chl a concentration averaged $3\,\mu g\,L^{-1}$ and recorded the highest peak compared to the other lakes (about $9\,\mu g\,L^{-1}$ at 10 m) before decreasing to $0.7\,\mu g\,L^{-1}$ below 15 m. Turbidity showed a large peak between 16 and 19 m. The pH showed a small decrease from 9 to 8.8 between the surface and 15 m depth. Based on the temperature profiles, epilimnion, metalimnion, and hypolimnion layers of La Preciosa in May 2019 broadly extended from 0–6, 6–15, and 15–46 m, respectively (Fig. 2).

The DIC concentration was constant throughout the water column at 13.3 mM, with an exception at 12.5 m, where it decreased to 11.5 mM (Fig. 3, Table S1). Calculated $p\mathrm{CO}_2$ at the surface represented about 2 times the atmospheric $p\mathrm{CO}_{2\,atm}$ (Table S2). The $\delta^{13}C_{DIC}$ decreased from about $0.5\,‰$ to $-0.36\,‰$ between the surface and the hypolimnion. The POC concentration decreased from ~ 0.06 mM in the epilimnion and metalimnion to 0.02 mM in the hypolimnion. Similarly, $(C:N)_{POM}$ decreased from ~ 11.2 in the epilimnion and metalimnion to 7.6 in the hypolimnion. The $\delta^{13}C_{POC}$ increased downward from $\sim -27\,‰$ to $-25\,‰$, with a peak of $-23.5\,‰$ at 15 m.

In the first 10 cm of sediments, $\delta^{13}C_{SOC}$ values increased downwards from $\sim -25.5\,‰$ to $-23.2\,‰$ and the C : N molar ratio from 9.8 to 11 (Figs. 3, 4; Table S3). Carbonates corresponded to aragonite and calcite and had a bulk C isotope

composition averaging 2.6‰ (Table S3). Porewaters from the 2016 La Preciosa core were not retrieved.

4.3 Lake Atexcac

Stratification of the Lake Atexcac water column was also very well defined (Fig. 2). Temperature decreased from ∼ 20.6 °C at the surface to reach 16 °C below 20 m. Conductivity showed the same trend with values between 13 and 12.8 mS cm^{-1} near the surface (salinity around 7.4 psu). Dissolved O_2 was slightly oversaturated at the lake surface (115 % or 7.6 mg L^{-1}), rapidly decreasing to 0 mg L^{-1} between ∼ 10 and 20 m, while ORP signal decreased below a depth of 22 m. Chl a averaged 1 µg L^{-1} and showed a narrow peak centered at around 16 m, reaching ∼ 2 µg L^{-1}. Turbidity showed a pronounced increase below 20 m, peaking at 23.3 m and returning to surface values at 26 m. The pH remained around 8.85 throughout the water column. Based on the temperature profiles, the epilimnion, metalimnion, and hypolimnion of Atexcac in May 2019 broadly extended from 0–10, 10–20, and 20–39 m, respectively (Fig. 2).

The DIC concentration was around 26 mM throughout the water column, except at 23 m, where it decreased to 24.2 mM (Fig. 3, Table S1). Calculated pCO$_2$ was about 5 times higher than the atmospheric pCO$_{2\,atm}$ (Table S2). The δ^{13}C$_{DIC}$ was stable around 0.4‰ in the epilimnion and metalimnion but increased to 0.9‰ at 23 m and reached 0.2‰ minimum values at the bottom of the lake. The POC concentration was ∼ 0.05 mM in the epilimnion and metalimnion, decreasing to 0.02 mM in the hypolimnion. The C : N molar ratio of POM showed the same depth profile, decreasing from ∼ 9.6 in the epilimnion and metalimnion to 6.6 in the hypolimnion (Fig. 3). The δ^{13}C$_{POC}$ showed minimum values in the epilimnion and metalimnion (−29.3‰ at 16 m) and increased to −26.5‰ in the hypolimnion.

Dissolved sulfate concentration was relatively stable at ∼ 2.51 mM throughout the water column but increased to 2.64 mM at 23 m. Dissolved Mn concentration was constant at 1 µM down to 16 m, before dropping to 0 at 23 m and increasing again to 2.35 µM at 30 m (Fig. 2; Table S4). Similar depth profiles were found for other heavy elements as well, including Cu, Sr, Ba, or Pb among others.

In the first 12 cm of sediments, DIC concentration in the porewater varied between ∼ 21 and 26 mM, and δ^{13}C$_{DIC}$ was around 0‰. Carbonates corresponded to aragonite and calcite and had a bulk C isotope composition between 2.1‰ and 2.6‰ (Table S3). Sedimentary organic matter had a δ^{13}C$_{SOC}$ averaging −26.8 ± 0.1‰ and a C : N molar ratio increasing from 8 to 10 (Figs. 3, 4; Table S3).

4.4 Lake Alchichica

The water column of Lake Alchichica showed a pronounced stratification compared to previous years at the same period (Figs. 2, S2; Lugo et al., 2000; Adame et al., 2008;

Macek et al., 2020). Temperature decreased from ∼ 20 °C at the surface to 15.5 °C at depths below 30 m. Conductivity showed the same trend with values between around 13.8 mS cm^{-1} (salinity decreasing from 7.9 to 7.8 psu). Dissolved O_2 was slightly oversaturated at the lake surface (112 % or 7.5 mg L^{-1}), rapidly decreasing to 0 mg L^{-1} between ∼ 10 and 20 m. The ORP followed a similar trend but decreasing below 30 m only. The offset between O_2 exhaustion and decrease of the ORP can be explained by the presence of other oxidant species and/or extended Chl a peaks (Supplement Text S1). Chl a averaged 2 µg L^{-1}, with a broad peak extending from ∼ 7 to 29 m (averaging 4 µg L^{-1}) and showing a narrow 6 µg L^{-1} maximum values at 23 m. Then, it decreased to minimum values of ∼ 0.5 µg L^{-1} in the lower water column. The pH remained constant at ∼ 9.2 over the whole water column. Based on the temperature profiles, the epilimnion, metalimnion and hypolimnion layers of Lake Alchichica in May 2019 extended from 0–10, 10–20, and 20–63 m, respectively (Fig. 2).

The DIC concentration was around 34.8 mM throughout the water column, except at 10 m where it decreased to 33 mM (Fig. 3; Table S1). Calculated pCO$_2$ was about 3 times higher than the atmospheric pCO$_{2\,atm}$ (Table S2). The δ^{13}C$_{DIC}$ decreased from 2‰ to ∼ 1.5‰ between 5 and 60 m depth (Fig. 4; Table S1). The POC concentration was ∼ 0.09 mM in the epilimnion and metalimnion, decreasing to 0.02 mM in the hypolimnion. The δ^{13}C$_{POC}$ increased from −26.5‰ in the top 30 m to −24.1‰ at 55 m. The C : N molar ratio of POM showed a similar profile with values around 10.5 down to 30 m, progressively decreasing towards 5.9 at 55 m (Fig. 3; Table S1).

In the first 12 cm of sediments, porewater DIC had a concentration of ∼ 35.5 mM, and δ^{13}C$_{DIC}$ decreased from 0.4‰ to −0.5‰. Solid carbonates were contained within several phases (aragonite, hydromagnesite, huntite, and calcite) and had a bulk C isotope composition around 4.6‰ (Table S3). Sedimentary organic matter had a δ^{13}C$_{SOC}$ increasing from −25.7‰ to −24.5‰ and a constant C : N molar ratio slightly higher than 10 (Figs. 3, 4; Table S3).

5 Discussion

5.1 Inorganic carbon: origins and implications of the alkalinity / DIC gradient

5.1.1 Sources of DIC and origin of the inter-lake alkalinity gradient

Salinity and DIC concentration gradually increase from Alberca de los Espinos (0.6 psu, 7 mM) to Alchichica (7.9 psu, 35 mM), while La Preciosa (1.15 psu, 13 mM) and Atexcac (7.44 psu, 26 mM) have intermediate values (Table 1 and S1). This trend matches the alkalinity gradient (with values of ∼ 8, 15, 32 and 47 meq L^{-1}, Fig. S3a) previously de-
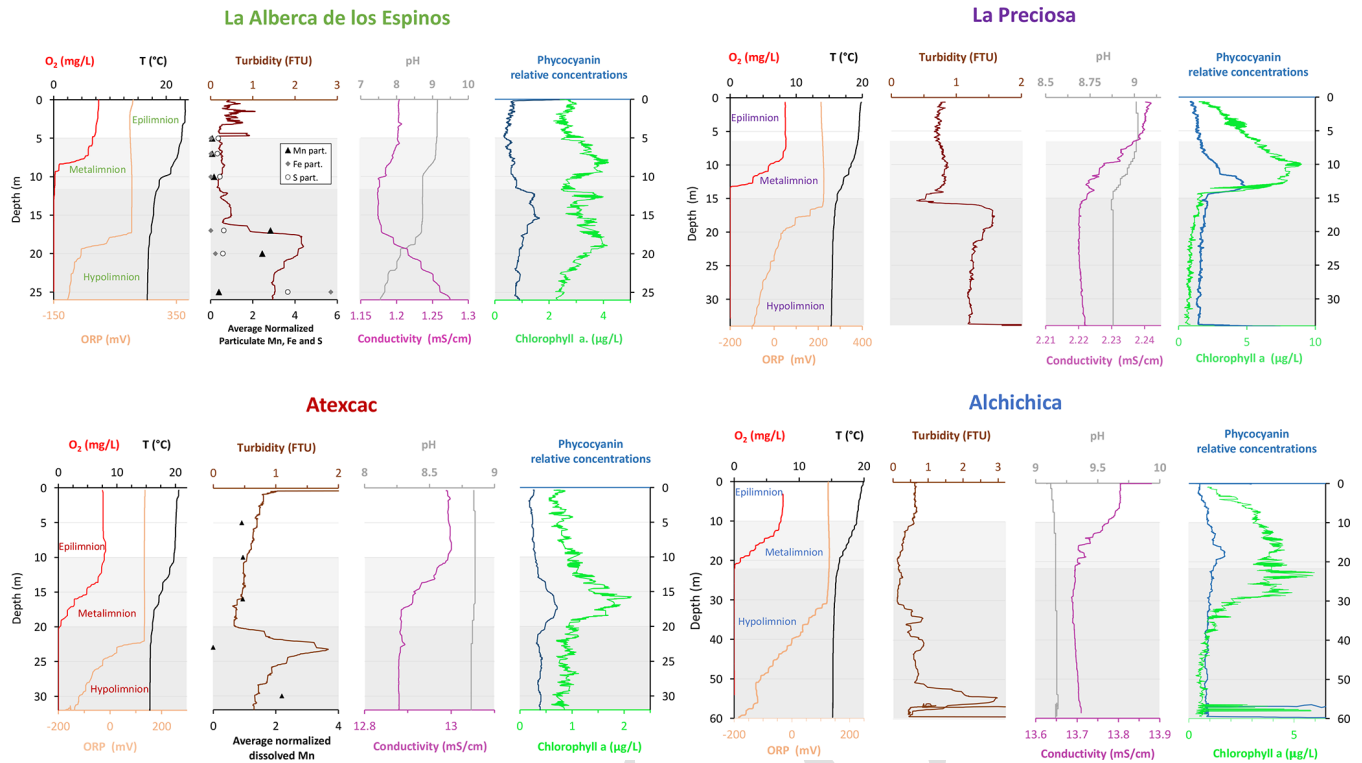
Figure 2. Physicochemical parameter depth profiles in Alberca de los Espinos, La Preciosa, Atexcac, and Alchichica in May 2019, including dissolved oxygen concentration (mg L^{-1}), water temperature (°C), oxidation-reduction potential (ORP, mV), turbidity (Formazin Turbidity Unit), pH, conductivity (mS cm^{-1}), phycocyanin, and chlorophyll *a* pigments (µg L^{-1}). Absolute values for phycocyanin concentrations were not determined, only relative variations are represented (with increasing concentrations to the right). Discrete concentration values of dissolved Mn in Atexcac and particulate Mn, Fe, and S in Alberca, normalized by their respective averages, are represented. Epilimnion, metalimnion, and hypolimnion layers are depicted for each lake according to temperature profiles. The three layers closely corresponded to oxygen-rich, oxygen-poor, and intermediate zones (except in La Preciosa where the oxycline was slightly thinner than the thermocline layer, ∼ 5 vs. 8 m).

scribed for these lakes (Zeyen et al., 2021), consistent with the fact that alkalinity is mainly composed of HCO$_3^-$ and CO$_3^{2-}$ ions in most natural waters. This alkalinity gradient may result from different concentration stages of an initial dilute alkaline water (Zeyen et al., 2021), ultimately controlled by differences in hydrological regime between the four lakes. In the SOB, the weathering of basaltic and andesitic bedrock (Armienta et al., 2008; Carrasco-Núñez et al., 2007; Lelli et al., 2021) and Cretaceous limestone (with $\delta^{13}C \approx 0 \pm 1\%$; Gonzales-Partida et al., 1993; Armstrong-Altrin et al., 2011) favors the inflow of more alkaline and DIC-concentrated groundwater than in Alberca, which lies on an essentially basaltic basement (Rendon-Lopez, 2008; Siebe et al., 2014; Zeyen et al., 2021). The SOB is currently experiencing higher rates of evaporation than precipitation (Alcocer, 2021), which may play an important role in concentrating solutes and decreasing the water level in La Preciosa, Atexcac, and Alchichica (Anderson and Stedmon, 2007; Zeyen et al., 2021). Substantial "sub-fossil" microbialite deposits emerge well above the current water level in lakes Atexcac and Alchichica, confirming this fall in wa-

ter level (∼ 15 m for Atexcac and ∼ 5 m for Alchichica). Scattered patches of microbialites emerge at La Preciosa (suggesting a water level decrease of ∼ 6 m). By contrast, emerged microbialites are virtually absent in Lake Alberca de los Espinos (Fig. S1).

Additional local parameters such as variable groundwater paths and fluxes (Furian et al., 2013; Mercedes-Martín et al., 2019; Milesi et al., 2020; Zeyen et al., 2021) most likely play a role in explaining some of the variation in DIC concentration between lakes. La Preciosa's water composition significantly differs from that of Atexcac and Alchichica, despite a similar geological context and climate (all are located within 50 km^2, Fig. 1). Groundwater in the SOB area becomes more saline as it flows towards the center of the basin and through the crater lakes (Silva Aguilera, 2019; Alcocer, 2021). Since groundwater flows through La Preciosa first, its ionic strength (including DIC concentration) increases as it enters Alchichica (Silva Aguilera, 2019; Alcocer, 2021; Lelli et al., 2021). Different regimes of volcanic CO$_2$ degassing into these crater lakes may also contribute to variation in the C mass balance and $\delta^{13}C_{DIC}$ values between
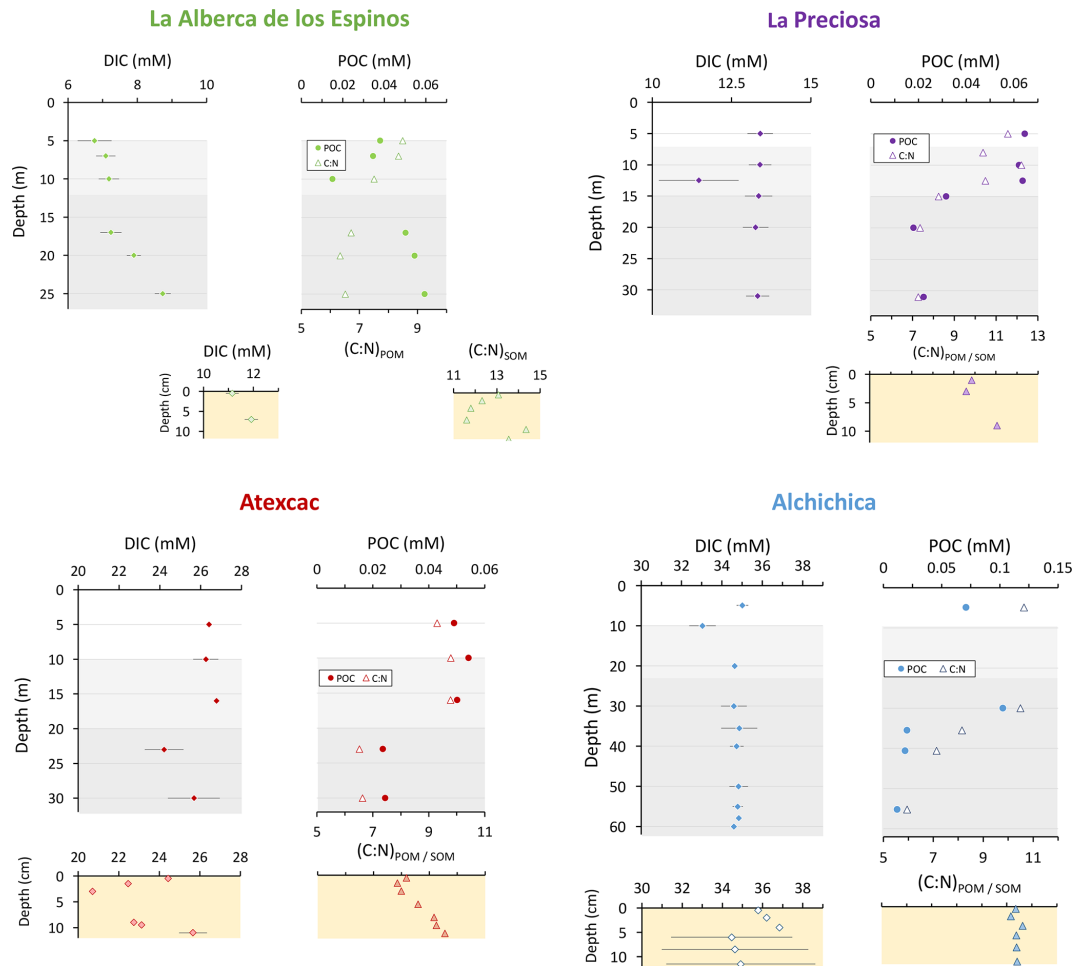
Figure 3. Concentrations in mmol L^{-1} (mM) of DIC, DOC, and POC and the sum of all three reservoirs; C : N molar ratios of POM as a function of depth in the water columns; and DIC concentrations in the surficial sediment porewaters and C : N molar ratios of sedimentary OM. Porewaters from La Preciosa's 2016 core were not retrieved.

the four lakes. Near the lakes from the SOB area, geothermal fluids derived from meteoric waters have been shown to interact with deep volcanic fluids as well as the calcareous basement rocks (Peiffer et al., 2018; Lelli et al., 2021). In the water column of Alberca, $\delta^{13}C_{total}$ averages $-4.8‰$ (Havas et al., 2023a TS4). This isotopic composition is very similar to signatures of mantle CO_2 (Javoy et al., 1986; Mason et al., 2017), which could buffer the overall C isotope composition of this lake. Alberca is located on top of a likely active normal fault (Siebe et al., 2012), favoring the ascent of volcanic gases.

Differences in the remineralization rate of organic carbon (OC) could also contribute to the heterogeneous DIC content among the lakes. However, assuming that all OC from the lakes ultimately remineralized into DIC, it would still represent only a small proportion of the total carbon (9 % for Alberca, $\sim$ 5 % for La Preciosa and Alchichica, and 16 % for Atexcac; Havas et al., 2023). From an isotopic mass balance perspective, Lake Alberca exhibits more negative $\delta^{13}C_{DIC}$

(and $\delta^{13}C_{Carb}$), slightly closer to OC signatures, whereas the $\delta^{13}C_{DIC}$ of the three SOB lakes lies very far from OC isotopic signatures (Fig. 4). Dense vegetation surrounds Alberca (Fig. S1), making it the only lake in this study where OC respiration could be a significant source of inorganic C to the water column (potentially influencing the P_{CO_2}, [DIC], and pH profiles described above).

In summary, a combination of very local and external environmental factors generates the contrasting water chemistries of the lakes, notably a gradient in their alkalinity and [DIC]. This chemical variability stems from the exact nature of the basement rocks, the distinct groundwater flow paths feeding the lakes, differences in evaporation rates, and potentially different volcanic CO_2 degassing regimes.
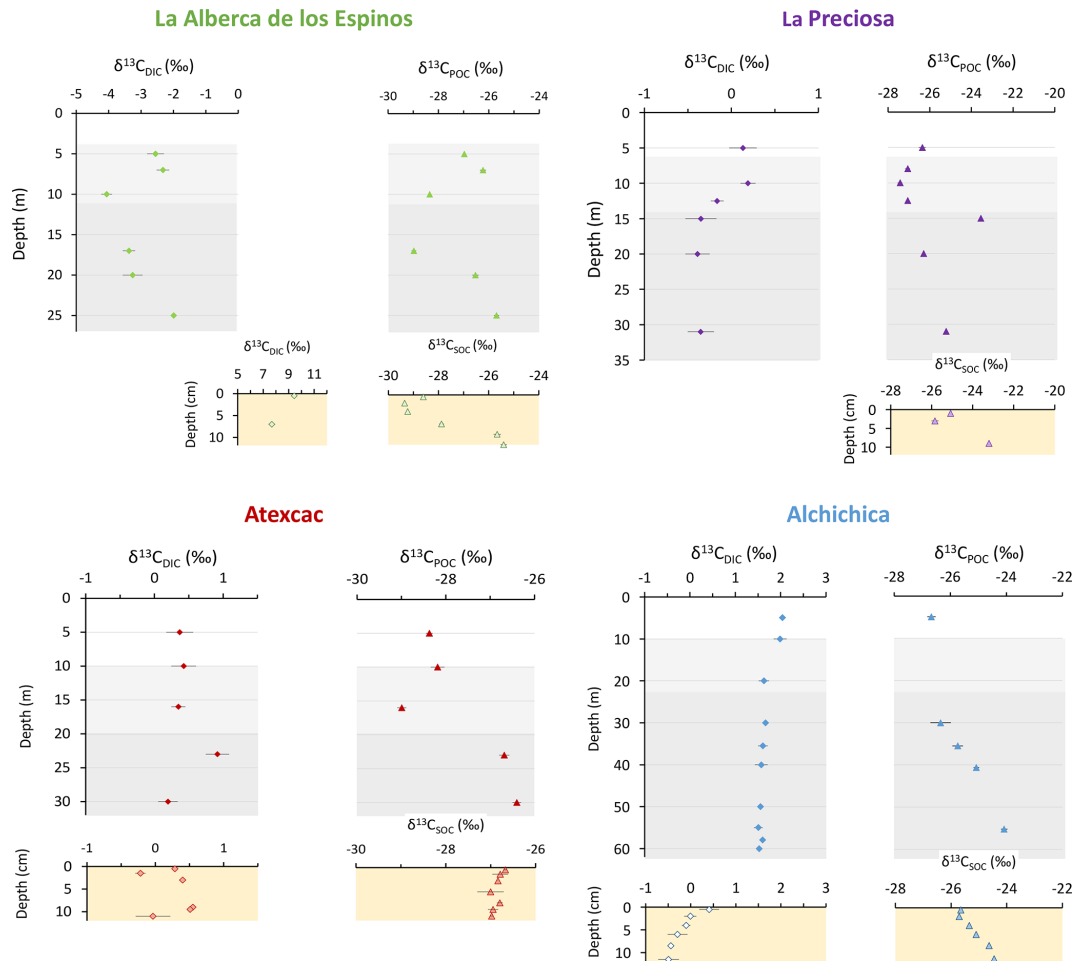
Figure 4. Isotopic compositions of DIC and POC reservoirs as a function of depth in the water columns, as well as isotopic compositions of the porewater DIC and total organic carbon from the surficial sediments.

5.1.2 Influence of alkalinity on physicochemical stratification in the four lakes

Stratified water columns can sustain strong physicochemical gradients, where a wide range of biogeochemical reactions impacting the C cycle can take place (e.g., Jézéquel et al., 2016). In the four lakes studied here, the evolution of pH with depth exemplifies the interplay between the alkalinity gradient, the physicochemical stratification of the lakes, and their respective C cycle. The pH shows a stratified profile in Alberca and La Preciosa but remains constant in Atexcac and Alchichica. The decline in pH at the oxycline of La Preciosa is associated with the decrease in POC and chlorophyll a concentrations and $\delta^{13}C_{DIC}$ values, reflecting the impact of oxygen respiration (i.e., carbon remineralization) at this depth (Figs. 2–4). In Alberca, the surface waters are markedly more alkaline than the bottom waters, with a two-step decrease in pH occurring at 8 and 17 m (with a total drop of 1.5 pH unit). As in La Preciosa, this pH decrease likely results from high OM respiration, although input of volcanic

acidic gases (e.g., dissolved CO_2 with $\delta^{13}C \sim -5\,‰$) might also contribute to the pH decrease in the bottom waters, reflected by negative $\delta^{13}C_{DIC}$ signatures and an increase of [DIC] and conductivity in the hypolimnion (Figs. 2 and 4). By contrast, while the same evidence for oxygen respiration ([POC], chlorophyll a) can be detected in the other two lakes, it does not impact their pH profile in a similar way (Fig. 2). This result suggests that the acidity generated by OM respiration (and possibly volcanic CO_2 degassing) is buffered by the much higher alkalinity measured in these two lakes.

External forcings such as lake hydrology and fluid sources thus impact the alkalinity buffering capacity of these lakes and influence the vertical pH profile of the water columns, which is particularly important considering the critical interplay between pH and biogeochemical reactions affecting the C cycle (e.g., Soetaert et al., 2007).

5.1.3 Sinks of DIC along the alkalinity gradient

Interplay between pH and sources of alkalinity and DIC in the lakes also has a strong impact on their C storage capacity, as it can result in different fluxes of the C sinks (inorganic and organic C precipitation and sedimentation, CO_2 degassing).

Alkaline pH can store large quantities of DIC because it favors the presence of HCO_3^- and CO_3^{2-} species over $H_2CO_3^*$ (the intermediate species between gaseous $CO_{2(g)}$ and bicarbonate/carbonate ions, defined here as the sum of H_2CO_3 and $CO_{2(aq)}$). Carbonate and bicarbonate ions represent over 99 % of total DIC in the four lakes (Table S2). In Alberca de los Espinos, the lake with the lowest DIC, the surface water pCO_2 is slightly lower than atmospheric $pCO_{2\,atm}$ (Table S2). By contrast, large amounts of CO_2 degas at the surface of the SOB lakes, as indicated by their elevated surface water pCO_2, from 2 to 5 times higher than atmospheric $pCO_{2\,atm}$ (Table S2). These different CO_2 degassing potentials are consistent with the notion that higher DIC concentrations favor CO_2 degassing through higher pCO_2 (e.g., Duarte et al., 2008). Although Alberca and Alchichica (the two end-members of the alkalinity gradient) have the same surface water pH, CO_2 degassing is 3 times higher at Alchichica for a given value of gas transfer velocity.

Another important C sink for these lakes is the precipitation of carbonate minerals, found in the microbialites and lake sediments. Lake alkalinity and the resulting mineral saturation index greatly influence the amount of C precipitated from the lake waters. Although the four lakes are supersaturated with aragonite, calcite, and the precursor-phase monohydrocalcite, they present highly contrasted amounts of carbonate deposits (Zeyen et al., 2021). The occurrence of microbialites increases along the alkalinity gradient, with limited presence at Alberca and more massive deposits at Atexcac and Alchichica (Zeyen et al., 2021; Fig. S1). Similarly, surficial sediments contain only 16 wt % for Alberca but from 40 wt % to 62 wt % carbonates for the SOB lakes (Table S3). Thus, the SOB lakes seem to bury more C than Alberca de los Espinos. Nonetheless, the data from May 2019 indicate that Alberca was the only one of the four lakes with a pCO_2 slightly lower than atmospheric $pCO_{2\,atm}$, thus representing a net sink of C. Classifying the three other lakes as net C sources or sinks – notably in order to see the influence of their respective position in the alkalinity gradient – will require a more detailed description of C in and out fluxes, since they all store and emit significant amounts of C (as organic and inorganic C deposits and via CO_2 degassing, respectively). However, such a C budget is out of the scope of the present study.

5.1.4 Isotopic signatures of inorganic C in the four lakes ($\delta^{13}C_{DIC}$ and $\delta^{13}C_{Carbonates}$)

The DIC isotopic composition of the lakes (between $\sim -3\,‰$ and $+2\,‰$ on average; Table S1) is consistent with the DIC sources described above. The lower $\delta^{13}C_{DIC}$ in Alberca is consistent with influence of remineralized OC and/or volcanic CO_2. The $\delta^{13}C_{DIC}$ in the SOB lakes suggests groundwater $\delta^{13}C_{DIC}$ values resulting from the dissolution of the Cretaceous limestone basement.

By controlling DIC speciation (H_2CO_3 / $CO_{2(aq)}$, HCO_3^-, CO_3^{2-}), pH also strongly influences $\delta^{13}C_{DIC}$. Indeed, there is a temperature-dependent fractionation of up to $10\,‰$ between the different DIC species (Emrich et al., 1970; Mook et al., 1974; Bade et al., 2004; Table S6). The Mexican lakes present $\delta^{13}C_{DIC}$ values that are common for lakes with a pH around 9 (Bade et al., 2004), where DIC is dominated by HCO_3^-. However, the pH values of the four lakes studied here are too similar to explain the significant difference between their $\delta^{13}C_{DIC}$ (Fig. 4; $p = 4.2 \times 10^{-3}$ for La Preciosa and Atexcac, which have the closest $\delta^{13}C_{DIC}$). Part of the variability of $\delta^{13}C_{DIC}$ among the lakes may result from their distinct evaporation stages, as the mean $\delta^{13}C_{DIC}$ values of the lakes broadly correlate with their salinity and alkalinity (Fig. S3b). Evaporation generally increases the $\delta^{13}C_{DIC}$ of residual waters by increasing lake pCO_2 and primary productivity, which bolsters CO_2 degassing and organic C burial, both having low $\delta^{13}C$ compared to DIC (e.g., Li and Ku, 1997; Talbot, 1990). Accordingly, the pCO_2 of Alberca is lower than that of the other lakes (Table S2). The $\delta^{13}C_{DIC}$ in lakes with lower DIC concentrations is expected to be more easily influenced by exchanges with other carbon reservoirs, such as organic carbon (through photosynthesis and respiration), or other DIC sources (e.g., depleted volcanic CO_2 or groundwater DIC), compared to buffered, high DIC lakes (Li and Ku, 1997). As a result, the low DIC and alkalinity concentration in Alberca features the lowest $\delta^{13}C_{DIC}$ of the four lakes, likely reflecting organic and/or volcanic C influence and thus higher responsiveness to biogeochemical processes of the inorganic C reservoir. By contrast, the three SOB lakes exhibit $\delta^{13}C_{DIC}$ with less internal variability, with a maximum amplitude of $0.7\,‰$ within a single water column.

Surficial sedimentary carbonates are in isotopic equilibrium with the $\delta^{13}C_{DIC}$ of the water columns, within the uncertainty of $\delta^{13}C_{DIC}$ measurement, and more specifically with the $\delta^{13}C_{DIC}$ values at the oxycline and thermocline of the lakes (Tables S6 and S7). The $\delta^{13}C_{DIC}$ at equilibrium with carbonates is estimated by correcting the carbonate C isotope composition ($\delta^{13}C_{Carb}$) by the fractionation value between DIC and the different carbonate mineralogies (Supplement Text S2). Therefore, the $\delta^{13}C_{Carb}$ also follows and reflects the alkalinity gradient, with the lowest $\delta^{13}C_{Carb}$ found in the surficial sediments of Alberca ($\sim -1.5\,‰$), intermediate values in La Preciosa and Atexcac ($\sim 2.5\,‰$), and the highest values in Alchichica ($\sim +4.6\,‰$) (Table S3).

In summary, although all four lakes present the same general structure and environmental conditions (i.e., tropical alkaline stratified crater lakes), external and local factors (e.g., hydrology, fluid sources, and stratification characteristics) re-

Table 2. Index for mathematical notations used in the text including C isotopic composition of a reservoir X ($\delta^{13}C_X$) and isotopic discrimination between the two carbon reservoirs X and Y ($\Delta^{13}C_{X-Y}$). In the main text, we report organic C isotope discrimination versus both bulk DIC ($\Delta^{13}C_{POC-DIC}$) – in a way to facilitate intercomparison studies and because it is the commonly reported raw measured data (Fry, 1996) – and calculated $CO_{2(aq)}$ (ε_{POC-CO_2}) in order to discuss the intrinsic isotopic fractionations associated with the lakes metabolic diversity. All C isotope values and fractionations are reported relative to the international standard VPDB (Vienna Pee Dee Belemnite).

Symbols	Mathematical expression	Signification
$\delta^{13}C_X$	$\left(\dfrac{\left(\frac{^{13}C}{^{12}C}\right)_X}{\left(\frac{^{13}C}{^{12}C}\right)_{VPDB}} - 1 \right) \times 1000$	Relative difference in $^{13}C : {}^{12}C$ isotopic ratio between a sample of a given C reservoir and the international standard "Vienna Pee Dee Bee", expressed in permil (‰). $\delta^{13}C_{total}$ represents the weighted average of $\delta^{13}C$ for all DIC and POC.
$\Delta^{13}C_{X-Y}$	$= \delta^{13}C_X - \delta^{13}C_Y \approx 1000 \ln \alpha_{X-Y}$	Apparent isotopic fractionation between two reservoirs "X" and "Y". Difference between their measured C isotope compositions approximating the fractionation α in permil.
$\varepsilon_{X\text{-}CO_2}$	$= (\alpha_{X\text{-}CO_2} - 1)1000 \approx \delta^{13}C_X - \delta^{13}C_{CO_2}$	Calculated isotopic fractionation between a reservoir "X" and $CO_{2(aq)}$. $\alpha_{X\text{-}CO_2}$ is calculated as $(\delta^{13}C_X + 1000)/(\delta^{13}C_{CO_2} + 1000)$, where $\delta^{13}C_X$ is measured and $\delta^{13}C_{CO_2}$ is computed based on DIC isotopic composition and speciation (see Supplement text S3).

sult in contrasting water chemistry compositions, which have a critical impact on the physicochemical depth profiles of each lake and their biogeochemical carbon cycle functioning. These external factors represent a first-order control on the size, isotopic composition, and responsiveness to biogeochemical processes of the inorganic C reservoir. Lakes with the highest alkalinity and DIC content will poorly record internal biological processes. Interestingly, C storage in mineral carbonates seems to be significant in watersheds where carbonate deposits pre-exist in the geological substratum (here, the Cretaceous limestone basement), providing more alkaline and C-rich sources.

5.2 Particulate organic carbon: from water column primary production to respiration recycling and sedimentary organic matter

5.2.1 Particulate organic C sources

Primary productivity by oxygenic photosynthesis in the upper water column

The C : N ratios of water column POM and bulk organic matter in the sediments of the four lakes ranged from 6 to 13 (Fig. 3), close to the phytoplankton Redfield ratio but much lower than land–plant ratios. Yet abundant vegetation covers the crater walls of Alberca and, to a lesser extent, of Atexcac, and some plant debris was found in the sediment cores of these two lakes. Its analysis resulted in high C : N ratios (between 24 and 68), typical of plant tissues and significantly higher than those of the bulk sediment and water column organic matter. Thus, the allochthonous organic carbon in these two lakes does not significantly contribute to their bulk organic signal. All four crater lakes are endorheic basins, with no surface water inflow or outflow, supporting the predominantly autochthonous origin of organic carbon sources (Alcocer et al., 2014), from planktonic autotrophic C fixation.

The importance of planktonic autotrophic C fixation as a major source of POC in the four lakes is further supported by the assessment of the isotopic discrimination between DIC and organic biomass, expressed as $\Delta^{13}C_{POC-DIC}$ and ε_{POC-CO_2} (Table 2). The $\Delta^{13}C_{POC-DIC}$ varies between $\sim -29‰$ and $-23‰$ (corresponding to ε_{POC-CO_2} between $\sim -19‰$ and $-13‰$) throughout the four water columns, within the typical range of planktonic oxygenic phototrophs (Pardue et al., 1976; Sirevag et al., 1977; Thomas et al., 2019). Yet these values exhibit variability – both within a single water column (up to 4.5‰) and among the four lakes (up to 6‰; Figs. 4 and 5). The $\Delta^{13}C_{POC-DIC}$ variability may reflect several abiotic and biotic factors.

Notably, lower DIC availability in Alberca and La Preciosa probably makes the carboxylation step less limiting during photosynthesis (e.g., O'Leary, 1988; Descolas-Gros and Fontungne, 1990; Fry, 1996), decreasing $|\varepsilon_{POC-CO_2}|$ in these lakes (between 14.5‰ and 17.7‰ at the peak of Chl a) compared to Atexcac and Alchichica (Fig. 5a; between 17.5‰ and 19.2‰). Lower $CO_{2(aq)}$ availability and/or higher reaction rates result in transport-limited rather than carboxylation-limited fixation, with smaller C isotope fractionation between POC and DIC (Pardue et al., 1976; Zohary et al., 1994; Fry, 1996; Close and Henderson, 2020). The isotopic fractionation associated with diffusion is much smaller than with carboxylation, and a higher proportion of the DIC entering the cells is converted into organic biomass (e.g., Fogel and Cifuentes, 1993). We consistently notice a correlation among the lakes between $a(CO_2)_{(aq)}$ (or [DIC]) and $|\varepsilon_{POC-CO_2}|$ at depths where oxygenic photosynthesis
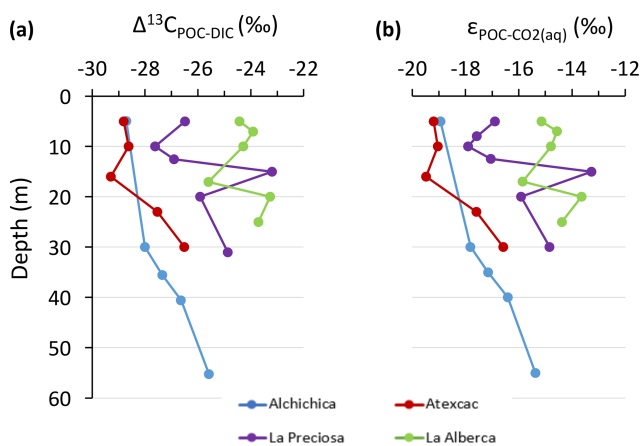
Figure 5. Isotopic fractionations between POC and DIC in the water columns of the four lakes, expressed as **(a)** $\Delta^{13}C_{x-y}$ and **(b)** ε_{POC-CO_2}. Refer to Table 2 for more detail about the Δ and ε notations.

peaks (Fig. 6). Furthermore, Alberca and La Preciosa are considered less oligotrophic than the two other lakes (Lugo et al., 1993; Vilaclara et al., 1993; Havas et al., 2023), with higher chlorophyll a contents and thus smaller $|\varepsilon_{POC-CO_2}|$ (Fig. 5). Higher water temperatures in Alberca de los Espinos (by $\sim 3\,°C$) could also partly contribute to a smaller $|\varepsilon_{POC-CO_2}|$ in this lake (Sackett et al., 1965; Pardue et al., 1976; Descolas-Gros and Fontugne, 1990).

Unlike $\delta^{13}C_{DIC}$, organic carbon isotope signatures do not evolve linearly with the alkalinity/salinity gradient, suggesting other lake- and microbial-specific controls on these signatures. These controls include diffusive or active uptake mechanisms, specific carbon fixation pathways, the fraction of intracellular inorganic carbon released out of the cells, cell size and geometry (Werne and Hollander, 2004, and references therein), and remineralization efficiency. Moreover, an increasing number of isotopic data have evidenced a significant variability of the isotopic fractionation achieved by different purified RuBisCO enzymes ($\varepsilon_{RuBisCO}$, Iñiguez et al., 2020) and even by a single RuBisCO form (Thomas et al., 2019). Thus, caution should be paid to the interpretation of the origin of small isotopic variations of the biomass in distinct environmental contexts because RuBisCO alone can be an important source of this variability (Thomas et al., 2019).

Primary production in the anoxic hypolimnion

Anoxygenic autotrophs commonly thrive in anoxic bottom waters of stratified water bodies (e.g., Pimenov et al., 2008; Zyakun et al., 2009; Posth et al., 2017; Fulton et al., 2018; Havig et al., 2018). They have been identified at different depths in the four Mexican lakes (Macek et al., 2020; Iniesto et al., 2022). In our samples collected during the stratification period, anoxygenic autotrophs appear to have a distinct impact on the C cycle of Alberca and Atexcac only. Lake Atex-

cac records a concomitant decrease in [DIC] and increase in $\delta^{13}C_{DIC}$ in the anoxic hypolimnion at 23 m, below the peak of Chl a, suggesting autotrophic C fixation by chemoautotrophy or anoxygenic photosynthesis. The calculated ε_{POC-CO_2} at 23 m ($-17.3\,‰$) is consistent with C isotope fractionation by purple- and green-sulfur-anoxygenic bacteria (PSB and GSB), while ε_{POC-CO_2} in Alberca's hypolimnion ($\sim -15\,‰$) is closer to GSB canonical signatures (Posth et al., 2017 and references therein) (Fig. 5b). In Alberca, anoxygenic primary productivity is suggested by increasing POC concentrations below the oxycline, showing a distinct isotopic signature (Figs. 4 and 5). We also observe a Chl a peak in the anoxic hypolimnion of this lake (Fig. 2), which likely represents a bias of the probe towards some bacteriochlorophyll pigments typical of GSB (see Supplement text S4). In Atexcac, C fixation by anoxygenic autotrophs at 23 m causes a shift in the DIC reservoir, while oxygenic photosynthesis at 16 m does not, suggesting that anaerobic autotrophs are the main autotrophic metabolisms in this lake (in terms of DIC uptake). In Alberca, the increase in [POC] to maximum values below the oxycline also supports the predominance of anoxygenic versus oxygenic autotrophy (Fig. 3), similar to other stratified water bodies exhibiting primary production clearly dominated by anoxygenic metabolisms (Fulton et al., 2018).

Lastly, at 23 m in Atexcac and 17 m in Alberca, we find a striking turbidity peak precisely where the redox potential and the concentration of dissolved Mn drops (Fig. 2). In Atexcac, the concentration of dissolved metals such as Cu, Pb, or Co also drops at 23 m (Fig. S4). In Alberca, a peak of particulate Mn concentration is detected at 15 m (Fig. 2; data unavailable for Atexcac). This peak is most likely explained by the precipitation of Mn mineral particles, where reduced bottom waters meet oxidative conditions prevailing in the upper waters. These oxidized Mn phases can be used as electron acceptors during chemoautotrophy (Havig et al., 2015; Knossow et al., 2015; Henkel et al., 2019; van Vliet et al., 2021). Even at a low particle density, such phases can catalyze abiotic oxidation of sulfide to sulfur compounds, which in turn can be used and further oxidized to sulfate by phototrophic or chemoautotrophic sulfur-oxidizing bacteria (van Vliet et al., 2021). Autotrophic sulfur oxidation is also consistent with the small increase in $[SO_4^{2-}]$ observed at 23 m in Atexcac (Table S4).

In summary, combined POC and DIC data allowed us to recognize the most representative autotrophic metabolisms in the Mexican lakes. The upper water columns are all dominated by oxygenic photosynthesis. Lower in the water columns, anoxygenic photosynthesis and/or chemoautotrophy were found to have a noticeable impact on POC and DIC reservoirs in Alberca and Atexcac only. Their activity was associated with metal element cycling. More specifically in Alberca, the anoxygenic phototrophs correspond to GSB.
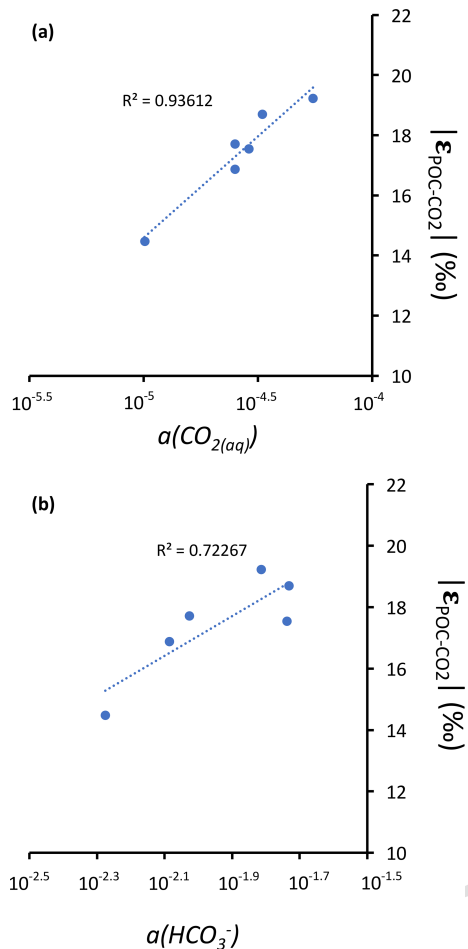
Figure 6. Cross plots of DIC species activities versus absolute values of calculated C isotopic fractionations between POC and CO_2 at depths of peak oxygenic photosynthesis where data were available (5 and 30 m for Alchichica, 16 m for Atexcac, 10 and 12.5 m for La Preciosa, and 7 m for Alberca). **(a)** Dissolved $CO_{2(aq)}$ activity and **(b)** bicarbonate activity as functions of $|\varepsilon_{POC-CO_2}|$ in permil plus linear correlation trends and corresponding R^2.

5.2.2 Sinks of particulate organic carbon: respiration and sedimentation

Aerobic respiration at the oxycline

At the oxycline of stratified water bodies, aerobic respiration of OM by heterotrophic organisms favors the transition from oxygenated upper layers to anoxic bottom waters. In the water column of the four lakes, $\Delta^{13}C_{POC-DIC}$ (and ε_{POC-CO_2}) show increasing values in the hypolimnion and especially below the chlorophyll a peaks (Figs. 2 and 5). The $\Delta^{13}C_{POC-DIC}$ trend correlates with increasing $\delta^{13}C_{POC}$, decreasing $(C:N)_{POM}$ ratios, and decreasing POC concentrations except in Alberca (Figs. 3 and 4). Decreasing POC concentrations near the oxycline and redoxcline are consistent with the fact that part of the upper primary production is de-

graded deeper in the water columns and/or that there is less primary production in the anoxic bottom waters. Increased $\delta^{13}C_{POC}$ in the hypolimnion of the lakes is consistent with heterotrophic activity and points out that POC at these depths could mainly record secondary production rather than being a residue of sinking degraded OM formed by primary production. Heterotrophic bacteria preferentially grow on available ^{13}C-enriched amino acids and sugars, thus becoming more enriched than their C source (Williams and Gordon, 1970; Hayes et al., 1989; Zohary et al., 1994; Briones et al., 1998; Lehmann et al., 2002; Jiao et al., 2010; Close and Henderson, 2020). The decrease in C : N ratios in the POM also reinforces this conclusion, since secondary heterotrophic bacteria biomass generally have C : N between 4 and 5 (Lehmann et al., 2002), whereas residual degraded OM from primary producers would carry higher C : N signatures (van Mooy et al., 2002; Buchan et al., 2014). These latter signatures are not recorded by POM in the lower water columns of the lakes (Fig. 3).

The $\delta^{13}C_{DIC}$ signatures in La Preciosa and Alchichica are consistent with the mineralization of OM, as they exhibit lower values below the oxycline than in surficial waters (Figs. 2 and 4). Similarly to what is observed in several other water bodies and notably stratified water columns such as the Black Sea (e.g., Fry et al., 1991), surface photosynthesis increases $\delta^{13}C_{DIC}$ by fixing light DIC, while respiration transfers light OC back to the DIC pool at depth. Such a decrease in $\delta^{13}C_{DIC}$ can also be seen in the oxycline of Lake Alberca between 7 and 10 m.

Influence of methanogenesis in Lake Alberca de los Espinos

Alberca shows the least saline and alkaline water column and most peculiar geochemical depth profiles among the four lakes. Notably, its [DIC] and $\delta^{13}C_{DIC}$ (the lowest of the studied lakes) increase from the lower metalimnion to the hypolimnion and further into the first cm of sediment porewaters, with $\delta^{13}C_{DIC}$ reaching almost 10‰ (Figs. 3, 4). The calculated CO_2 partial pressure (P_{CO_2}) increases downward from slightly less than $1\times P_{CO_2\text{-atm}}$ near the lake surface up to almost $40\times$ at the bottom of the lake (Table S2).

While the increase of [POC] at depth may contribute to the observed $\delta^{13}C_{DIC}$ increase, by mass balance, it should also lower the [DIC] instead of increasing it. Similarly, the sinking of POC at depth followed by its remineralization into DIC cannot explain the $\delta^{13}C_{DIC}$ trend, since it would lower the $\delta^{13}C_{DIC}$ in the hypolimnion (Fig. 4). Overall, these observations require that a significant source of inorganic ^{13}C-rich carbon fuels the bottom waters of Alberca de los Espinos. The source of heavy carbon most likely results from methanogenesis, which consumes organic carbon in the sediments and produces ^{13}C-depleted methane and ^{13}C-rich carbon dioxide diffusing upward in the water column (i.e., acetoclastic methanogenesis, dominant in lacustrine contexts;

Whiticar et al., 1986). Methanogenesis, as an "alternative" OM remineralization pathway, would be favored in Alberca because it is relatively rich in OM (notably with high [DOC], Havas et al., 2023) and depleted in SO_4^{2-} (Wittkop et al., 2014; Birgel et al., 2015; Cadeau et al., 2020) compared to the other three Mexican lakes. Based on the $\delta^{13}C_{SOC}$ and porewater $\delta^{13}C_{DIC}$, we can tentatively calculate the methane isotopic signature in Alberca (see Supplement Text S5). The resulting $\delta^{13}C_{CH_4}$ in the first 10 cm of sediments is between −59‰ and −57‰, which is consistent with the range of isotopic composition of methane after biogenic methanogenesis (Whiticar et al., 1986).

Upward-diffusing methane may be either (i) partly lost from the lake's surface (i.e., escaping the system) by degassing or (ii) totally retained in the water column by complete oxidation (either abiotically by oxygenated surface waters or biologically by methanotrophic organisms). The oxidation of CH_4 in the water column should lead to the formation of ^{13}C-depleted carbon dioxide that would mix back with the lake DIC (and notably with heavy methanogenic CO_2 produced at depth) and/or ^{13}C-depleted biomass (as POC or SOC) if it occurs through methanotrophy. Thus, the net effect of combined methanogenesis and methane oxidation is expected to (i) generate a $\delta^{13}C_{DIC}$ gradient from high to low values between the sediment porewaters and the oxycline as proposed elsewhere (Assayag et al., 2008; Wittkop et al., 2014) and (ii) progressively lower sedimentary $\delta^{13}C_{SOC}$ in the case of methanotrophy. Abiotic oxidation of methane by dioxygen is consistent with the observation that $\delta^{13}C_{DIC}$ decreases from porewaters ($\sim +10$‰) to the oxycline (-4‰), reaching minimum values where dissolved O_2 starts to appear (Fig. 2). Microbial anaerobic oxidation of methane (AOM) could occur at the 17 m depth through Mn-oxide reduction (Cai et al., 2021; Cheng et al., 2021) and possibly bacterial sulfate reduction closer to the water-sediment interface, as inferred for the surficial sediments of meromictic Lake Cadagno (Posth et al., 2017). Indeed, we observe a net increase of particulate Fe and S concentrations at a depth of 25 m and a peak of solid sulfide minerals in the surficial sediments (Fig. S5). However, $\delta^{13}C_{SOC}$ and $\delta^{13}C_{POC}$ are far from calculated $\delta^{13}C_{CH_4}$, suggesting that AOM is not a major process in the bottom lake waters and surface sediments (Lehmann et al., 2004) and thus that methanotrophy is not the main CH_4 oxidation pathway in Lake Alberca.

Alternatively, if some portion of the methane escaped oxidation and degassed out of the lake, $\delta^{13}C_{DIC}$ would likely be driven to extreme positive values with time (Gu et al., 2004; Hassan, 2014; Birgel et al., 2015; Cadeau et al., 2020). Methane escape is not consistent with the average $\delta^{13}C_{DIC}$ in Alberca (~ -3‰; Fig. 4), unless an additional counterbalancing source of DIC to this lake exists. This source of DIC could be volcanic CO_2 degassing (see Sect. 5.1.1). Such a contribution may maintain the lake's average $\delta^{13}C_{total}$ close to a mantle isotopic signature and notably away from extreme positive values if CH_4 escape dominated. It is also possible

that volcanic CO_2 degassing is coupled with methanogenesis by CO_2 reduction in addition to the acetoclastic type described above.

Although volcanic CO_2 could be an important source in the C mass balance of Lake Alberca, we note that it cannot explain the very positive $\delta^{13}C_{DIC}$ in the sediment porewaters alone, thus bolstering the identification of methanogenesis. Importantly, this methane cycle is cryptic to the sediment record, as it is evidenced in the dissolved inorganic C phase but not in the sedimentary organic matter or carbonates. This is a consequence of the lake's stratified nature, where the location of carbonate precipitation and methane production is decoupled.

Transfer of OM from the water column to the surficial sediments

The OC content in the first 12 cm of the sediment cores from the four lakes ranges from 1 wt % to 13 wt % (Table S3). These concentrations are relatively elevated considering the predominantly autochthonous nature of OC and the oligotrophic conditions in these lakes (Alcocer et al., 2014; Havas et al., 2023). In Lake Alchichica, the recent OC burial flux in the sediment was estimated to represent between 15 and 26 g yr^{-1} m^{-2} (Alcocer et al., 2014). These values are within the range observed for small lakes around the world (Mulholland and Elwood, 1982; Dean and Gorham, 1998; Mendonça et al., 2017), though most of them receive allochthonous OM inputs. Different factors can favor the preservation of OM, including lower respiration and oxidation rates due to anoxic bottom waters and scarce benthic biota and/or high sedimentation rates (Alcocer et al., 2014). Anaerobic respiration clearly occurs in the four lakes to some extent, as detailed for Alberca and as seen in the surficial sediment data of the other lakes as well (decreasing $\delta^{13}C_{DIC}$ in Alchichica, increasing C : N ratio in Atexcac and La Preciosa; Table S3). Nonetheless, the anoxic conditions prevailing in the hypolimnion most of the year are significantly more favorable to OM preservation than oxic conditions (Sobek et al., 2009; Kuntz et al., 2015). While the yearly mixing oxidizes most of the water column during the winter, it also generates a bloom of diatoms which fosters OM production (through shuttling up of bio-essential nutrients such as N and Si) and development of anoxia (e.g., Adame et al., 2008). In Alchichica, the large size of some of the phytoplankton was also suggested to favor OM preservation (Adame et al., 2008; Ardiles et al., 2011). Because bacterial sulfate reduction (BSR) is a major remineralization pathway in SO_4-rich environments (e.g., Jørgensen, 1982), the low sulfate content in Alberca probably favors the preservation of high TOC in the sediments, even though appreciable BSR rates may occur in this lake (see discussion above and Fig. S5), similarly to other sulfate-poor environments due to rapid S cycling (e.g., Vuillemin et al., 2016; Friese et al., 2021). Again, a complete mass balance of these lakes'

C fluxes will be required to estimate their net C emission or sequestration behavior.

Although the nature and geochemical signatures of the OM that deposits in the sediments may vary throughout the year, it is interesting to infer from what part(s) of the water column surficial sedimentary OM comes during the stratified seasons. In the three lakes from the SOB, $\delta^{13}C_{SOC}$ and $(C:N)_{SOM}$ signatures of the surficial sedimentary OM lie somewhere between POM signatures from the upper water column and from the hypolimnion (Figs. 3, 4). More precisely, in Alchichica, the most surficial $\delta^{13}C_{SOC}$ and $(C:N)_{SOM}$ signatures ($-25.7‰$ and $10.4‰$, respectively) are much closer to values recorded in the upper water column ($\sim -26.5‰$ and $10.5‰$, respectively), implying that the upper oxygenic photosynthesis production is primarily recorded. It is consistent with previous studies, suggesting that most of the phytoplankton biomass being exported is composed of diatoms (Ardiles et al., 2011). In Lake Atexcac, however, $\delta^{13}C_{SOC}$ and $(C:N)_{SOM}$ signatures ($\sim -26.8‰$ and 8, respectively) are closer to values recorded in the hypolimnion ($\sim -26.5‰$ and $6.5‰$, respectively), suggesting that SOM (sedimentary organic matter) records mostly the anaerobic primary production.

In Alberca, surficial $\delta^{13}C_{SOC}$ is markedly more negative (by $\sim 2‰$ to $3‰$) than the deepest and shallowest water column values (Fig. 4) but close to what is recorded at the redoxcline depth of 17 m. However, the $(C:N)_{SOM}$ values are much higher than what is measured anywhere in the water column, which is consistent with OM remineralization by sulfate-reduction and methanogenesis in the sediments of this lake. Therefore, OM biogeochemical signatures in the surficial sediments of Alberca could be strongly influenced by early diagenesis occurring at the water-sediment interface – despite favorable conditions for OM preservation.

In summary, the OM depositing at the bottom of these stratified lakes does not always record geochemical signatures from the same layers of the water columns and can be modified by very early diagenesis. It does not necessarily record the signatures of primary production by oxygenic photosynthesis from the upper column. For example, in Lake Atexcac, sedimentary OM records primary production by anoxygenic photosynthesis, even though POC concentration is highest in the upper water column. This result highlights the diversity of geochemical signatures that can stem from continental environments despite their geographical, geological, and climatic proximity. A deeper understanding of the OM transfer process from water column to sediment will require more detailed analyses and comparison of the different OM pigments and molecules and could have strong implications for the interpretation of the fossil record in deep anoxic time.

6 Conclusions and summary

The carbon cycles of four stratified alkaline crater lakes were described and compared based on the concentration and isotopic compositions of DIC and POC in the water columns and surficial (~ 10 cm) sedimentary carbonates and organic carbon. Overall our study shows the wide diversity of geochemical signatures found in continental stratified environments despite similar geological and climatic contexts. We identify different regimes of C cycling in the four lakes due to different biogeochemical reactions related to slight environmental and ecological variations. In more detail, we show the following.

– External abiotic factors, such as the hydrological regime and the inorganic C sources in the lakes, control their alkalinity and, thus, the buffering capacity of their waters. In turn, these differences in buffering capacity constrain variations in pH along the stratified water columns, as well as the inorganic C isotope signatures recorded in the water columns and sediments of the lakes. The $\delta^{13}C_{carb}$ reflects the abiotic factors generating the alkalinity gradient, but it is poorly representative of biological processes in lakes with high alkalinity. The external environmental factors further impact the C mass balance of the lakes with probable consequences on their net C-emitting or C-sequestering status.

– Based on POC and DIC concentrations and isotopic compositions, combined with physicochemical parameters, we are able to identify the activity of oxygenic photosynthesis and aerobic respiration in the four lakes studied. Anoxygenic photosynthesis and/or chemoautotrophy are also evidenced in two of the lakes, but their POC and DIC signatures can be equivocal.

– Methanogenesis is evidenced in the surficial sediments of the OM-rich Lake Alberca de los Espinos and influences the geochemical signatures lower in the water column. However, it is recorded only in analyses of porewater dissolved species but not imprinted in the sedimentary archives (OM and carbonates).

– The SOM geochemical signatures of these stratified lakes do not all record the same "biogeochemical layers" of the water column (e.g., anaerobic vs. aerobic metabolisms) and, in some cases, can be greatly modified by early diagenesis.

Data availability. The data are publicly accessible at https://doi.org/10.26022/IEDA/112943 (Havas et al., 2023b).

Supplement. The supplement related to this article is available online at: https://doi.org/10.5194/bg-20-1-2023-supplement.

Author contributions. RH and CT designed the study in a project directed by PLG, KB, and CT. CT, MI, DJ, DM, RT, PLG, and KB collected the samples in the field. RH carried out the measurements for the C data, DJ carried out the physicochemical parameter probe measurements, and EM provided data for trace and major elements. RH and CT analyzed the data. RH wrote the paper with important contributions from all co-authors.

Competing interests. The contact author has declared that none of the authors has any competing interests.

Acknowledgements. The authors thank Anne-Lise Santoni, Elodie Cognard, Théophile Cocquerez, and the GISMO platform (Biogéosciences, Université Bourgogne Franche-Comté, UMR CNRS 6282, France). We thank Céline Liorzou and Bleuenn Guéguen for the analyses at the Pôle Spectrométrie Océan (Laboratoire Géo-Océan, Brest, France) and Laure Cordier for ion chromatography analyses at IPGP (France). We thank Nelly Assayag and Pierre Cadeau for their help on the AP 2003 at IPGP. We warmly thank Carmela Chateau-Smith for improving the syntax and clarity of the manuscript.

Financial support. This research has been supported by the Agence Nationale de la Recherche (grant no. ANR-18-CE02-0013-02).

Review statement. This paper was edited by Tina Treude and reviewed by two anonymous referees.

References

Adame, M. F., Alcocer, J., and Escobar, E.: Size-fractioned phytoplankton biomass and its implications for the dynamics of an oligotrophic tropical lake, Freshw. Biol., 53, 22–31, https://doi.org/10.1111/j.1365-2427.2007.01864.x, 2008.

Ader, M., Macouin, M., Trindade, R. I. F., Hadrien, M.-H., Yang, Z., Sun, Z., and Besse, J.: A multilayered water column in the Ediacaran Yangtze platform? Insights from carbonate and organic matter paired $\delta^{13}C$, Earth Planet. Sc. Lett., 288, 213–22, https://doi.org/10.1016/j.epsl.2009.09.024, 2009.

Aharon, P.: Redox stratification and anoxia of the early Precambrian oceans: Implications for carbon isotope excursions and oxidation events, Precambrian Res., 173, 207–222, https://doi.org/10.1016/j.precamres.2005.03.008, 2005.

Alcocer, J.: Lake Alchichica Limnology, Springer Nature, https://doi.org/10.1007/978-3-030-79096-7, 2021.

Alcocer, J., Ruiz-Fernández, A. C., Escobar, E., Pérez-Bernal, L. H., Oseguera, L. A., and Ardiles-Gloria, V.: Deposition, burial and sequestration of carbon in an oligotrophic, tropical lake, J.

Limnol., 73, 223–235, https://doi.org/10.4081/jlimnol.2014.783, 2014.

Anderson, N. J. and Stedmon, C. A.: The effect of evapoconcentration on dissolved organic carbon concentration and quality in lakes of SW Greenland, Freshw. Biol., 52, 280–289, https://doi.org/10.1111/j.1365-2427.2006.01688.x, 2007.

Ardiles, V., Alcocer, J., Vilaclara, G., Oseguera, L. A., and Velasco, L.: Diatom fluxes in a tropical, oligotrophic lake dominated by large-sized phytoplankton, Hydrobiologia, 679, 77–90, https://doi.org/10.1007/s10750-011-0853-7, 2012.

Armienta, M. A., Vilaclara, G., De la Cruz-Reyna, S., Ramos, S., Ceniceros, N., Cruz, O., Aguayo, A., and Arcega-Cabrera, F.: Water chemistry of lakes related to active and inactive Mexican volcanoes, J. Volcanol. Geotherm. Res., 178, 249–258, https://doi.org/10.1016/j.jvolgeores.2008.06.019, 2008.

Armstrong-Altrin, J. S., Madhavaraju, J., Sial, A. N., Kasper-Zubillaga, J. J., Nagarajan, R., Flores-Castro, K., and Rodríguez, J. L.: Petrography and stable isotope geochemistry of the cretaceous El Abra Limestones (Actopan), Mexico: Implication on diagenesis, J. Geol. Soc. India, 77, 349–359, https://doi.org/10.1007/s12594-011-0042-3, 2011.

Assayag, N., Rivé, K., Ader, M., Jézéquel, D., and Agrinier, P.: Improved method for isotopic and quantitative analysis of dissolved inorganic carbon in natural water samples, Rapid Commun. Mass Spectrom., 20, 2243–2251, https://doi.org/10.1002/rcm.2585, 2006.

Assayag, N., Jézéquel, D., Ader, M., Viollier, E., Michard, G., Prévot, F., and Agrinier, P.: Hydrological budget, carbon sources and biogeochemical processes in Lac Pavin (France): Constraints from $\delta^{18}O$ of water and $\delta^{13}C$ of dissolved inorganic carbon, Appl. Geochem., 23, 2800–2816, https://doi.org/10.1016/j.apgeochem.2008.04.015, 2008.

Bade, D. L., Carpenter, S. R., Cole, J. J., Hanson, P. C., and Hesslein, R. H.: Controls of $\delta^{13}C$-DIC in lakes: Geochemistry, lake metabolism, and morphometry, Limnol. Oceanogr., 49, 1160–1172, https://doi.org/10.4319/lo.2004.49.4.1160, 2004.

Bekker, A., Holmden, C., Beukes, N. J., Kenig, F., Eglinton, B., and Patterson, W. P.: Fractionation between inorganic and organic carbon during the Lomagundi (2.22–2.1 Ga) carbon isotope excursion, Earth Planet. Sc. Lett., 271, 278–291, https://doi.org/10.1016/j.epsl.2008.04.021, 2008.

Birgel, D., Meister, P., Lundberg, R., Horath, T. D., Bontognali, T. R. R., Bahniuk, A. M., de Rezende, C. E., Vasconcelos, C., and McKenzie, J. A.: Methanogenesis produces strong ^{13}C enrichment in stromatolites of Lagoa Salgada, Brazil: a modern analogue for Palaeo-/Neoproterozoic stromatolites?, Geobiology, 13, 245–266, https://doi.org/10.1111/gbi.12130, 2015.

Briones, E. E., Alcocer, J., Cienfuegos, E., and Morales, P.: Carbon stable isotopes ratios of pelagic and littoral communities in Alchichica crater-lake, Mexico, Int. J. Salt Lake Res., 7, 345–355, https://doi.org/10.1007/BF02442143, 1998.

Buchan, A., LeCleir, G. R., Gulvik, C. A., and González, J. M.: Master recyclers: features and functions of bacteria associated with phytoplankton blooms, Nat. Rev. Microbiol., 12, 686–698, https://doi.org/10.1038/nrmicro3326, 2014.

Cadeau, P., Jézéquel, D., Leboulanger, C., Fouilland, E., Le Floc'h, E., Chaduteau, C., Milesi, V., Guélard, J., Sarazin, G., Katz, A., d'Amore, S., Bernard, C., and Ader, M.: Carbon isotope evidence for large methane emissions to the Proterozoic atmosphere, Sci.

Rep., 10, 18186, https://doi.org/10.1038/s41598-020-75100-x, 2020.

Cai, C., Li, K., Liu, D., John, C.M., Wang, D., Fu, B., Fakhraee, M., He, H., Feng, L., and Jiang, L.: Anaerobic oxidation of methane by Mn oxides in sulfate-poor environments, Geology, 49, 761–766, https://doi.org/10.1130/G48553.1, 2021.

Carrasco-Núñez, G., Ort, M. H., and Romero, C.: Evolution and hydrological conditions of a maar volcano (Atexcac crater, Eastern Mexico), J. Volcanol. Geotherm. Res., 159, 179–197, https://doi.org/10.1016/j.jvolgeores.2006.07.001, 2007.

Chako Tchamabé, B., Carrasco-Núñez, G., Miggins, D. P., and Németh, K.: Late Pleistocene to Holocene activity of Alchichica maar volcano, eastern Trans-Mexican Volcanic Belt, J. South Am. Earth Sci., 97, 102404, https://doi.org/10.1016/j.jsames.2019.102404, 2020.

Cheng, C., Zhang, J., He, Q., Wu, H., Chen, Y., Xie, H., and Pavlostathis, S. G.: Exploring simultaneous nitrous oxide and methane sink in wetland sediments under anoxic conditions, Water Res., 194, 116958, https://doi.org/10.1016/j.watres.2021.116958, 2021.

Close, H. G. and Henderson, L. C.: Open-Ocean Minima in δ^{13}C Values of Particulate Organic Carbon in the Lower Euphotic Zone, Front. Mar. Sci., 7, 540165, https://doi.org/10.3389/fmars.2020.540165, 2020.

Crowe, S. A., Katsev, S., Leslie, K., Sturm, A., Magen, C., Nomosatryo, S., Pack, M. A., Kessler, J. D., Reeburgh, W. S., Roberts, J. A., González, L., Douglas Haffner, G., Mucci, A., Sundby, B., and Fowle, D. A.: The methane cycle in ferruginous Lake Matano: Methane cycle in ferruginous Lake Matano, Geobiology, 9, 61–78, https://doi.org/10.1111/j.1472-4669.2010.00257.x, 2011.

Dean, W. E. and Gorham, E.: Magnitude and significance of carbon burial in lakes, reservoirs, and peatlands, Geology, 26, 535–538, https://doi.org/10.1130/0091-7613(1998)026<0535:MASOCB>2.3.CO;2, 1998.

Descolas-Gros, C. and Fontungne, M.: Stable carbon isotope fractionation by marine phytoplankton during photosynthesis, Plant Cell Environ., 13, 207–218, https://doi.org/10.1111/j.1365-3040.1990.tb01305.x, 1990.

Duarte, C. M., Prairie, Y. T., Montes, C., Cole, J. J., Striegl, R., Melack, J., and Downing, J. A.: CO_2 emissions from saline lakes: A global estimate of a surprisingly large flux, J. Geophys. Res.-Biogeo., 113, G4, https://doi.org/10.1029/2007JG000637, 2008.

Emrich, K., Ehhalt, D. H., and Vogel, J. C.: Carbon isotope fractionation during the precipitation of calcium carbonate, Earth Planet. Sc. Lett., 8, 363–371, https://doi.org/10.1016/0012-821X(70)90109-3, 1970.

Ferrari, L., Orozco-Esquivel, T., Manea, V., and Manea, M.: The dynamic history of the Trans-Mexican Volcanic Belt and the Mexico subduction zone, Tectonophysics, 522/523, 122–149, https://doi.org/10.1016/j.tecto.2011.09.018, 2012.

Fogel, M. L. and Cifuentes, L. A.: Isotope Fractionation during Primary Production, in: Organic Geochemistry, Topics in Geobiology, edited by: Engel, M. H. and Macko, S. A., Springer US, Boston, MA, 73–98, https://doi.org/10.1007/978-1-4615-2890-6_3, 1993.

Friese, A., Bauer, K., Glombitza, C., Ordoñez, L., Ariztegui, D., Heuer, V.B., Vuillemin, A., Henny, C., Nomosatryo, S., Simister, R., Wagner, D., Bijaksana, S., Vogel, H., Melles, M., Russell, J. M., Crowe, S. A., and Kallmeyer, J.: Organic matter mineralization in modern and ancient ferruginous sediments, Nat. Commun., 12, 2216, https://doi.org/10.1038/s41467-021-22453-0, 2021.

Fry, B.: ^{13}C / ^{12}C fractionation by marine diatoms, Mar. Eco. Prog. Ser., 134, 283–294, https://doi.org/10.3354/meps134283, 1996.

Fry, B., Jannasch, H. W., Molyneaux, S. J., Wirsen, C. O., Muramoto, J. A., and King, S.: Stable isotope studies of the carbon, nitrogen and sulfur cycles in the Black Sea and the Cariaco Trench, Deep-Sea Res., 38, S1003–S1019, https://doi.org/10.1016/S0198-0149(10)80021-4, 1991.

Fulton, J. M., Arthur, M. A., Thomas, B., and Freeman, K. H.: Pigment carbon and nitrogen isotopic signatures in euxinic basins, Geobiology, 16, 429–445, https://doi.org/10.1111/gbi.12285, 2018.

Furian, S., Martins, E. R. C., Parizotto, T. M., Rezende-Filho, A. T., Victoria, R. L., and Barbiero, L.: Chemical diversity and spatial variability in myriad lakes in Nhecolândia in the Pantanal wetlands of Brazil, Limnol. Oceanogr., 58, 2249–2261, https://doi.org/10.4319/lo.2013.58.6.2249, 2013.

Gérard, E., Ménez, B., Couradeau, E., Moreira, D., Benzerara, K., Tavera, R., and López-García, P.: Specific carbonate–microbe interactions in the modern microbialites of Lake Alchichica (Mexico), ISME J., 7, 1997–2009. https://doi.org/10.1038/ismej.2013.81, 2013.

Gonzales-Partida, E., Barragan-R, R. M., and Nieva-G, D.: Analisis geoquimico-isotopico de las especies carbonicas del fluido geotermico de Los Humeros, Puebla, México, Geofis. Int., 32, 299–309, https://doi.org/10.22201/igeof.00167169p.1993.32.2.563, 1993.

Gröger, J., Franke, J., Hamer, K., and Schulz, H. D.: Quantitative Recovery of Elemental Sulfur and Improved Selectivity in a Chromium-Reducible Sulfur Distillation, Geostand. Geoanal. Res., 33, 17–27, https://doi.org/10.1111/j.1751-908X.2009.00922.x, 2009.

Gu, B., Schelske, C. L., and Hodell, D. A.: Extreme ^{13}C enrichments in a shallow hypereutrophic lake: Implications for carbon cycling, Limnol. Oceanogr., 49, 1152–1159, https://doi.org/10.4319/lo.2004.49.4.1152, 2004.

Hassan, K. M.: Isotope geochemistry of Swan Lake Basin in the Nebraska Sandhills, USA: Large ^{13}C enrichment in sediment-calcite records, Geochemistry, 74, 681–690, https://doi.org/10.1016/j.chemer.2014.03.004, 2014.

Havig, J. R., Hamilton, T. L., McCormick, M., McClure, B., Sowers, T., Wegter, B., and Kump, L. R.: Water column and sediment stable carbon isotope biogeochemistry of permanently redox-stratified Fayetteville Green Lake, New York, USA, Limnol. Oceanogr., 63, 570–587, https://doi.org/10.1002/lno.10649, 2018.

Havig, J. R., McCormick, M. L., Hamilton, T. L., and Kump, L. R.: The behavior of biologically important trace elements across the oxic/euxinic transition of meromictic Fayetteville Green Lake, New York, USA, Geochim. Cosmochim. Ac., 165, 389–406, https://doi.org/10.1016/j.gca.2015.06.024, 2015.

Havas, R., Thomazo, C., Iniesto, M., Jézéquel, D., Moreira, D., Tavera, R., Caumartin, J., Muller, E., López-García, P., and Benzerara, K.: The hidden role of dissolved organic carbon in the

biogeochemical cycle of carbon in modern redox-stratified lakes, Biogeosciences, in press, 10.5194/egusphere-2023-23, 2023a.

Havas, R., Thomazo, C., Iniesto, M., Jezequel, D., Moreira, D., Tavera, R., Caumartin, J., Muller, E., Lopez Garcia, P., and Benzerara, K.: Carbon isotopes and alkalinity gradient for biogeochemical processes in modern stratified lakes v. 2, Version 1.0., Interdisciplinary Earth Data Alliance (IEDA) [data set], https://doi.org/10.26022/IEDA/112943, 2023b.

Hayes, J. M., Popp, B. N., Takigiku, R., and Johnson, M. W.: An isotopic study of biogeochemical relationships between carbonates and organic carbon in the Greenhorn Formation, Geochim. Cosmochim. Ac., 53, 2961–2972, https://doi.org/10.1016/0016-7037(89)90172-5, 1989.

Hayes, J. M., Strauss, H., and Kaufman, A. J.: The abundance of ^{13}C in marine organic matter and isotopic fractionation in the global biogeochemical cycle of carbon during the past 800 Ma, Chem. Geol., 161, 103–125, https://doi.org/10.1016/S0009-2541(99)00083-2, 1999.

Henkel, J. V., Dellwig, O., Pollehne, F., Herlemann, D. P. R., Leipe, T., and Schulz-Vogt, H. N.: A bacterial isolate from the Black Sea oxidizes sulfide with manganese(IV) oxide, P. Natl. Acad. Sci. USA, 116, 12153–12155, https://doi.org/10.1073/pnas.1906000116, 2019.

Hurley, S. J., Wing, B. A., Jasper, C. E., Hill, N. C., and Cameron, J. C.: Carbon isotope evidence for the global physiology of Proterozoic cyanobacteria, Sci. Adv., 7, eabc8998, https://doi.org/10.1126/sciadv.abc8998, 2021.

Iniesto, M., Moreira, D., Benzerara, K., Muller, E., Bertolino, P., Tavera, R., and López-García, P.: Rapid formation of mature microbialites in Lake Alchichica, Mexico, Environ. Microbiol. Rep., 13, 600–605, https://doi.org/10.1111/1758-2229.12957, 2021a.

Iniesto, M., Moreira, D., Reboul, G., Deschamps, P., Benzerara, K., Bertolino, P., Saghaï, A., Tavera, R., and López-García, P.: Core microbial communities of lacustrine microbialites sampled along an alkalinity gradient, Environ. Microbiol., 23, 51–68, https://doi.org/10.1111/1462-2920.15252, 2021b.

Iniesto, M., Moreira, D., Benzerara, K., Reboul, G., Bertolino, P., Tavera, R., and López-García, P.: Planktonic microbial communities from microbialite-bearing lakes sampled along a salinity-alkalinity gradient, Limnol. Oceanogr. lno., 67, 12233, https://doi.org/10.1002/lno.12233, 2022.

Iñiguez, C., Capó-Bauçà, S., Niinemets, Ü., Stoll, H., Aguiló-Nicolau, P., and Galmés, J.: Evolutionary trends in RuBisCO kinetics and their co-evolution with CO_2 concentrating mechanisms, Plant J., 101, 897–918, https://doi.org/10.1111/tpj.14643, 2020.

Javoy, M., Pineau, F., and Delorme, H.: Carbon and nitrogen isotopes in the mantle, Chem. Geol., 57, 41–62, https://doi.org/10.1016/0009-2541(86)90093-8, 1986.

Jézéquel, D., Michard, G., Viollier, E., Agrinier, P., Albéric, P., Lopes, F., Abril, G., and Bergonzini, L.: Carbon Cycle in a Meromictic Crater Lake: Lake Pavin, France, in: Lake Pavin: History, Geology, Biogeochemistry, and Sedimentology of a Deep Meromictic Maar Lake, edited by: Sime-Ngando, T., Boivin, P., Chapron, E., Jezequel, D., and Meybeck, M., Springer International Publishing, Cham, 185–203, https://doi.org/10.1007/978-3-319-39961-4_11, 2016.

Jiao, N., Herndl, G. J., Hansell, D. A., Benner, R., Kattner, G., Wilhelm, S. W., Kirchman, D. L., Weinbauer, M. G., Luo, T., Chen, F., and Azam, F.: Microbial production of recalcitrant dissolved organic matter: long-term carbon storage in the global ocean, Nat. Rev. Microbiol., 8, 593–599, https://doi.org/10.1038/nrmicro2386, 2010.

Jørgensen, B. B.: Mineralization of organic matter in the sea bed—the role of sulphate reduction, Nature, 296, 643–645, https://doi.org/10.1038/296643a0, 1982.

Karhu, J. A. and Holland, H. D.: Carbon isotopes and the rise of atmospheric oxygen, Geology, 24, 867, https://doi.org/10.1130/0091-7613(1996)024<0867:CIATRO>2.3.CO;2, 1996.

Klawonn, I., Van den Wyngaert, S., Parada, A. E., Arandia-Gorostidi, N., Whitehouse, M. J., Grossart, H.-P., and Dekas, A. E.: Characterizing the "fungal shunt": Parasitic fungi on diatoms affect carbon flow and bacterial communities in aquatic microbial food webs, P. Natl. Acad. Sci. USA, 118, e2102225118, https://doi.org/10.1073/pnas.2102225118, 2021.

Knossow, N., Blonder, B., Eckert, W., Turchyn, A. V., Antler, G., and Kamyshny, A.: Annual sulfur cycle in a warm monomictic lake with sub-millimolar sulfate concentrations, Geochem. Trans., 16, 7, https://doi.org/10.1186/s12932-015-0021-5, 2015.

Krissansen-Totton, J., Buick, R., and Catling, D. C.: A statistical analysis of the carbon isotope record from the Archean to Phanerozoic and implications for the rise of oxygen, Am. J. Sci., 315, 275–316. https://doi.org/10.2475/04.2015.01, 2015.

Kuntz, L. B., Laakso, T. A., Schrag, D. P., and Crowe, S. A.: Modeling the carbon cycle in Lake Matano, Geobiology, 13, 454–461, https://doi.org/10.1111/gbi.12141, 2015.

Lehmann, M. F., Bernasconi, S. M., Barbieri, A., and McKenzie, J. A.: Preservation of organic matter and alteration of its carbon and nitrogen isotope composition during simulated and in situ early sedimentary diagenesis, Geochim. Cosmochim. Ac., 66, 3573–3584, https://doi.org/10.1016/S0016-7037(02)00968-7, 2002.

Lehmann, M. F., Bernasconi, S. M., McKenzie, J. A., Barbieri, A., Simona, M., and Veronesi, M.: Seasonal variation of the δC and δN of particulate and dissolved carbon and nitrogen in Lake Lugano: Constraints on biogeochemical cycling in a eutrophic lake, Limnol. Oceanogr, 49, 415–429. https://doi.org/10.4319/lo.2004.49.2.0415, 2004.

Lelli, M., Kretzschmar, T. G., Cabassi, J., Doveri, M., Sanchez-Avila, J. I., Gherardi, F., Magro, G., and Norelli, F.: Fluid geochemistry of the Los Humeros geothermal field (LHGF – Puebla, Mexico): New constraints for the conceptual model, Geothermics, 90, 101983, https://doi.org/10.1016/j.geothermics.2020.101983, 2021.

Li, H.-C. and Ku, T.-L.: δ^{13}C–δ^{18}C covariance as a paleohydrological indicator for closed-basin lakes, Palaeogeogr. Palaeocl., 133, 69–80, https://doi.org/10.1016/S0031-0182(96)00153-8, 1997.

Logan, G. A., Hayes, J. M., Hieshima, G. B., and Summons, R. E.: Terminal Proterozoic reorganization of biogeochemical cycles, Nature, 376, 53–56, https://doi.org/10.1038/376053a0, 1995.

Lorenz, V.: On the growth of maars and diatremes and its relevance to the formation of tuff rings, Bull. Volcanol., 48, 265–274. https://doi.org/10.1007/BF01081755, 1986.

Lugo, A., Alcocer, J., Sanchez, M. R., and Escobar, E.: Trophic status of tropical lakes indicated by littoral protozoan assemblages, Internationale Vereinigung für theoretische

und angewandte Limnologie: Verhandlungen, 25, 4441–443, https://doi.org/10.1080/03680770.1992.11900159, 1993.

Lugo, A., Alcocer, J., Sánchez, M. del R., Escobar, E., and Macek, M.: Temporal and spatial variation of bacterioplankton abundance in a tropical, warm-monomictic, saline lake: Alchichica, Puebla, Mexico, Internationale Vereinigung für theoretische und angewandte Limnologie: Verhandlungen, 27, 2968–2971, https://doi.org/10.1080/03680770.1998.11898217, 2000.

Lyons, T. W., Reinhard, C. T., and Planavsky, N. J.: The rise of oxygen in Earth's early ocean and atmosphere, Nature, 506, 307–315, https://doi.org/10.1038/nature13068, 2014.

Macek, M., Medina, X. S., Picazo, A., Peštová, D., Reyes, F. B., Hernández, J. R. M., Alcocer, J., Ibarra, M. M., and Camacho, A.: Spirostomum teres: A Long Term Study of an Anoxic-Hypolimnion Population Feeding upon Photosynthesizing Microorganisms, Acta Protozool., 59, 13–38, https://doi.org/10.4467/16890027AP.20.002.12158, 2020.

Mason, E., Edmonds, M., and Turchyn, A. V.: Remobilization of crustal carbon may dominate volcanic arc emissions, Science, 357, 290–294, https://doi.org/10.1126/science.aan5049, 2017.

Mendonça, R., Müller, R. A., Clow, D., Verpoorter, C., Raymond, P., Tranvik, L. J., and Sobek, S.: Organic carbon burial in global lakes and reservoirs, Nat. Commun., 8, 1694, https://doi.org/10.1038/s41467-017-01789-6, 2017.

Mercedes-Martín, R., Ayora, C., Tritlla, J., and Sánchez-Román, M.: The hydrochemical evolution of alkaline volcanic lakes: a model to understand the South Atlantic Pre-salt mineral assemblages, Earth-Sci. Rev., 198, 102938, https://doi.org/10.1016/j.earscirev.2019.102938, 2019.

Milesi, V. P., Debure, M., Marty, N. C. M., Capano, M., Jézéquel, D., Steefel, C., Rouchon, V., Albéric, P., Bard, E., Sarazin, G., Guyot, F., Virgone, A., Gaucher, É. C., and Ader, M.: Early Diagenesis of Lacustrine Carbonates in Volcanic Settings: The Role of Magmatic CO_2 (Lake Dziani Dzaha, Mayotte, Indian Ocean), ACS Earth Space Chem., 4, 363–378, https://doi.org/10.1021/acsearthspacechem.9b00279, 2020.

Mook, W. G., Bommerson, J. C., and Staverman, W. H.: Carbon isotope fractionation between dissolved bicarbonate and gaseous carbon dioxide, Earth Planet. Sc. Lett., 22, 169–176, https://doi.org/10.1016/0012-821X(74)90078-8, 1974.

Mulholland, P. J. and Elwood, J. W.: The role of lake and reservoir sediments as sinks in the perturbed global carbon cycle, Tellus A, 34, 490–499, https://doi.org/10.1111/j.2153-3490.1982.tb01837.x, 1982.

O'Leary, M. H.: Carbon Isotopes in Photosynthesis, BioScience, 38, 328–336, https://doi.org/10.2307/1310735, 1988.

Pardue, J. W., Scalan, R. S., Van Baalen, C., and Parker, P. L.: Maximum carbon isotope fractionation in photosynthesis by blue-green algae and a green alga, Geochim. Cosmochim. Ac., 40, 309–312, https://doi.org/10.1016/0016-7037(76)90208-8, 1976.

Peiffer, L., Carrasco-Núñez, G., Mazot, A., Villanueva-Estrada, R. E., Inguaggiato, C., Bernard Romero, R., Rocha Miller, R., and Rojas, J. H.: Soil degassing at the Los Humeros geothermal field (Mexico), J. Volcanol. Geotherm. Res., 356, 163–174, https://doi.org/10.1016/j.jvolgeores.2018.03.001, 2018.

Petrash, D. A., Steenbergen, I. M., Valero, A., Meador, T. B., Paèes, T., and Thomazo, C.: Aqueous system-level processes and prokaryote assemblages in the ferruginous and sulfate-rich bottom waters of a post-mining lake, Biogeosciences, 19, 1723–1751, https://doi.org/10.5194/bg-19-1723-2022, 2022.

Pimenov, N. V., Lunina, O. N., Prusakova, T. S., Rusanov, I. I., and Ivanov, M. V.: Biological fractionation of stable carbon isotopes at the aerobic/anaerobic water interface of meromictic water bodies, Microbiology, 77, 751–759, https://doi.org/10.1134/S0026261708060131, 2008.

Posth, N. R., Bristow, L. A., Cox, R. P., Habicht, K. S., Danza, F., Tonolla, M., Frigaard, N.-U., and Canfield, D. E.: Carbon isotope fractionation by anoxygenic phototrophic bacteria in euxinic Lake Cadagno, Geobiology, 15, 798–816, https://doi.org/10.1111/gbi.12254, 2017.

Rendon-Lopez, M. J.: Limnologia fisica del lago crater los Espinos, Municipio de Jiménez Michoacan, Universidad Michoacana de San Nicolas de Hidalgo, INIRENA-UMSNH, 1–107, 2008.

Ridgwell, A. and Arndt, S.: Chap. 1 – Why Dissolved Organics Matter: DOC in Ancient Oceans and Past Climate Change, in: Biogeochemistry of Marine Dissolved Organic Matter, 2nd Edn., edited by: Hansell, D. A. and Carlson, C. A., Academic Press, Boston, 1–20, https://doi.org/10.1016/B978-0-12-405940-5.00001-7, 2015.

Sackett, W. M., Eckelmann, W. R., Bender, M. L., and Bé, A. W. H.: Temperature Dependence of Carbon Isotope Composition in Marine Plankton and Sediments, Science, 148, 235–237, https://doi.org/10.1126/science.148.3667.235, 1965.

Saghaï, A., Zivanovic, Y., Moreira, D., Benzerara, K., Bertolino, P., Ragon, M., Tavera, R., López-Archilla, A. I., and López-García, P.: Comparative metagenomics unveils functions and genome features of microbialite-associated communities along a depth gradient: Comparative metagenomics of microbialites from Lake Alchichica, Environ. Microbiol., 18, 4990–5004, https://doi.org/10.1111/1462-2920.13456, 2016.

Saini, J. S., Hassler, C., Cable, R., Fourquez, M., Danza, F., Roman, S., Tonolla, M., Storelli, N., Jacquet, S., Zdobnov, E. M., and Duhaime, M. B.: Microbial loop of a Proterozoic ocean analogue, bioRxiv, 2021-08, https://doi.org/10.1101/2021.08.17.456685, 2021.

Satkoski, A. M., Beukes, N. J., Li, W., Beard, B. L., and Johnson, C. M.: A redox-stratified ocean 3.2 billion years ago, Earth Planet. Sc. Lett., 430, 43–53, https://doi.org/10.1016/j.epsl.2015.08.007, 2015.

Schidlowski, M.: Carbon isotopes as biogeochemical recorders of life over 3.8 Ga of Earth history: evolution of a concept, Precambrian Res., 106, 117–134, https://doi.org/10.1016/S0301-9268(00)00128-5, 2001.

Schiff, S. L., Tsuji, J. M., Wu, L., Venkiteswaran, J. J., Molot, L. A., Elgood, R. J., Paterson, M. J., and Neufeld, J. D.: Millions of Boreal Shield Lakes can be used to Probe Archaean Ocean Biogeochemistry, Sci. Rep., 7, 46708, https://doi.org/10.1038/srep46708, 2017.

Siebe, C., Guilbaud, M.-N., Salinas, S., and Chédeville-Monzo, C.: Eruption of Alberca de los Espinos tuff cone causes transgression of Zacapu lake ca. 25,000 yr BP in Michoacán, México, Presented at the IAS 4IMC Conference, Auckland, New Zeland, 74–75, https://www.researchgate.net/publication/283927123 (last access: 8 June 2023), 2012.

Siebe, C., Guilbaud, M.-N., Salinas, S., Kshirsagar, P., Chevrel, M. O., Jiménez, A. H., and Godínez, L.: Monogenetic volcanism of the Michoacán-Guanajuato Volcanic Field: Maar craters

of the Zacapu basin and domes, shields, and scoria cones of the Tarascan highlands (Paracho-Paricutin region), Presented at the Pre-meeting field guide for the 5th international Maar Conference, Querétaro, México, 1–37, https://www.researchgate.net/profile/Pooja_Kshirsagar/publication/275951848 (last access: 8 June 2023), 2014.

Sigala, I., Caballero, M., Correa-Metrio, A., Lozano-García, S., Vázquez, G., Pérez, L., and Zawisza, E.: Basic limnology of 30 continental waterbodies of the Transmexican Volcanic Belt across climatic and environmental gradients, Bol. Soc. Geológica Mex., 69, 313–370, https://doi.org/10.18268/BSGM2017v69n2a3, 2017.

Silva Aguilera, R. A.: Análisis del descenso del nivel de agua del Lago Alchichica, Puebla, México (Tesis de Maestría), Universidad Nacional Autónoma de México, Coordinación General de Estudios de Posgrado, UNAM, https://repositorio.unam.mx/contenidos/3534827 (last access: 6 June 2023), 2019.

Sirevag, R., Buchanan, B. B., Berry, J. A., and Troughton, J. H.: Mechanisms of CO_2 Fixation in Bacterial Photosynthesis Studied by the Carbon Isotope Fractionation Technique, Arch. Microbiol., 112, 35–38, https://doi.org/10.1007/BF00446651, 1977.

Sobek, S., Durisch-Kaiser, E., Zurbrügg, R., Wongfun, N., Wessels, M., Pasche, N., and Wehrli, B.: Organic carbon burial efficiency in lake sediments controlled by oxygen exposure time and sediment source, Limnol. Oceanogr., 54, 2243–2254, https://doi.org/10.4319/lo.2009.54.6.2243, 2009.

Soetaert, K., Hofmann, A. F., Middelburg, J. J., Meysman, F. J. R., and Greenwood, J.: The effect of biogeochemical processes on pH, Mar. Chem., 105, 30–51, https://doi.org/10.1016/j.marchem.2006.12.012, 2007.

Talbot, M. R.: A review of the palaeohydrological interpretation of carbon and oxygen isotopic ratios in primary lacustrine carbonates, Chem. Geol. Isot. Geosci., Sect. 80, 261–279, https://doi.org/10.1016/0168-9622(90)90009-2, 1990.

Thomas, P. J., Boller, A. J., Satagopan, S., Tabita, F. R., Cavanaugh, C. M., and Scott, K. M.: Isotope discrimination by form IC RubisCO from *Ralstonia eutropha* and *Rhodobacter sphaeroides*, metabolically versatile members of "*Proteobacteria*" from aquatic and soil habitats, Environ. Microbiol., 21, 72–80, https://doi.org/10.1111/1462-2920.14423, 2019.

Ussiri, D. A. N. and Lal, R.: Carbon Sequestration for Climate Change Mitigation and Adaptation, Springer International Publishing, Cham, https://doi.org/10.1007/978-3-319-53845-7, 2017.

Van Mooy, B. A. S., Keil, R. G., and Devol, A. H.: Impact of suboxia on sinking particulate organic carbon: Enhanced carbon flux and preferential degradation of amino acids via denitrification, Geochim. Cosmochim. Ac., 66, 457–465, https://doi.org/10.1016/S0016-7037(01)00787-6, 2002.

van Vliet, D. M., Meijenfeldt, F. A. B., Dutilh, B. E., Villanueva, L., Sinninghe Damsté, J. S., Stams, A. J. M., and Sánchez-Andrea, I.: The bacterial sulfur cycle in expanding dysoxic and euxinic marine waters, Environ. Microbiol., 23, 2834–2857, https://doi.org/10.1111/1462-2920.15265, 2021.

Vilaclara, G., Chávez, M., Lugo, A., González, H., and Gaytán, M.: Comparative description of crater-lakes basic chemistry in Puebla State, Mexico, Internationale Vereinigung für theoretische und angewandte Limnologie: Verhandlungen, 25, 435–440, https://doi.org/10.1080/03680770.1992.11900158, 1993.

Vuillemin, A., Friese, A., Alawi, M., Henny, C., Nomosatryo, S., Wagner, D., Crowe, S. A., and Kallmeyer, J.: Geomicrobiological features of ferruginous sediments from Lake Towuti, Indonesia, Front. Microbiol., 7, 1007, https://doi.org/10.3389/fmicb.2016.01007, 2016.

Wang, S., Yeager, K. M., and Lu, W.: Carbon isotope fractionation in phytoplankton as a potential proxy for pH rather than for $[CO_{2(aq)}]$: Observations from a carbonate lake, Limnol. Oceanogr., 61, 1259–1270, https://doi.org/10.1002/lno.10289, 2016.

Werne, J. P. and Hollander, D. J.: Balancing supply and demand: controls on carbon isotope fractionation in the Cariaco Basin (Venezuela) Younger Dryas to present, Mar. Chem., 92, 275–293, https://doi.org/10.1016/j.marchem.2004.06.031, 2004.

Whiticar, M. J., Faber, E., and Schoell, M.: Biogenic methane formation in marine and freshwater environments: CO_2 reduction vs. acetate fermentation – Isotope evidence, Geochim. Cosmochim. Ac., 50, 693–709, https://doi.org/10.1016/0016-7037(86)90346-7, 1986.

Williams, P. M. and Gordon, L. I.: Carbon-13: carbon-12 ratios in dissolved and particulate organic matter in the sea, Deep-Sea Res. Oceanogr., 17, 19–27, https://doi.org/10.1016/0011-7471(70)90085-9, 1970.

Wittkop, C., Teranes, J., Lubenow, B., and Dean, W. E.: Carbon- and oxygen-stable isotopic signatures of methanogenesis, temperature, and water column stratification in Holocene siderite varves, Chem. Geol., 389, 153–166, https://doi.org/10.1016/j.chemgeo.2014.09.016, 2014.

Zeyen, N., Benzerara, K., Beyssac, O., Daval, D., Muller, E., Thomazo, C., Tavera, R., López-García, P., Moreira, D., and Duprat, E.: Integrative analysis of the mineralogical and chemical composition of modern microbialites from ten Mexican lakes: What do we learn about their formation?, Geochim. Cosmochim. Ac., 305, 148–184, https://doi.org/10.1016/j.gca.2021.04.030, 2021.

Zohary, T., Erez, J., Gophen, M., Berman-Frank, I., and Stiller, M.: Seasonality of stable carbon isotopes within the pelagic food web of Lake Kinneret, Limnol. Oceanogr., 39, 1030–1043, https://doi.org/10.4319/lo.1994.39.5.1030, 1994.

Zyakun, A. M., Lunina, O. N., Prusakova, T. S., Pimenov, N. V., and Ivanov, M. V.: Fractionation of stable carbon isotopes by photoautotrophically growing anoxygenic purple and green sulfur bacteria, Microbiology, 78, 757–768, https://doi.org/10.1134/S0026261709060137, 2009.

Remarks from the typesetter

TS1   Please check all figures again concenring the changes.

TS2   Please give an explanation of why this needs to be changed. We have to ask the handling editor for approval. Thanks.

TS3   Please give an explanation of why this needs to be changed. We have to ask the handling editor for approval. Thanks.

TS4   The two companion papers will be linked online over a link at the respective manuscript website and will be named "Companion Paper". Please see the following example https://mr.copernicus.org/articles/4/153/2023/. Thank you for yoru understanding.